Methane dynamics in the Weddell Sea determined via stable isotope ratios and CFC-11

Katja U. Heeschen,[1,2] Robin S. Keir,[3] Gregor Rehder,[3] Olaf Klatt,[4,5] and Erwin Suess[3]

Received 18 September 2003; revised 11 February 2004; accepted 1 April 2004; published 5 June 2004.

[1] The physical, chemical/biological processes that control the methane dynamics in the Weddell Sea are revealed by the distributions of methane (CH_4), its stable carbon isotope ratio, $\delta^{13}C$-CH_4, and the conservative transient tracer, chlorofluorocarbon-11 (CFC-11, CCl_3F). In general, a nearly linear correlation between CH_4 and CFC-11 concentrations was observed. Air-sea exchange is the major source of methane to this region, and the distribution of methane is controlled mainly by mixing between surface water and methane-poor Warm Deep Water. A significant influence of methane oxidation over the predominant two end-member mixing was only found in the Weddell Sea Bottom Water (WSBW) of the deep central Weddell Basin, where the turnover time of methane appears to be about 20 years. Mixing also controls most of the $\delta^{13}C$-CH_4 distribution, but lighter than expected carbon isotopic ratios occur in the deep WSBW of the basin. From box model simulations, it appears that this ''anomaly'' is due to methane oxidation with a low kinetic isotope fractionation of about 1.004. The surface waters in the Weddell Sea and the Antarctic Circumpolar Current showed a general methane undersaturation of 6 to 25% with respect to the atmospheric mixing ratio. From this undersaturation and model-derived air-sea exchange rates, we estimate a net uptake of CH_4 of roughly -0.5 μmol m^{-2} d^{-1} during austral autumn. *INDEX TERMS:* 4207 Oceanography: General: Arctic and Antarctic oceanography; 4805 Oceanography: Biological and Chemical: Biogeochemical cycles (1615); 4820 Oceanography: Biological and Chemical: Gases; 4870 Oceanography: Biological and Chemical: Stable isotopes; *KEYWORDS:* chlorofluorocarbon, methane, Weddell Sea

Citation: Heeschen, K. U., R. S. Keir, G. Rehder, O. Klatt, and E. Suess (2004), Methane dynamics in the Weddell Sea determined via stable isotope ratios and CFC-11, *Global Biogeochem. Cycles*, *18*, GB2012, doi:10.1029/2003GB002151.

1. Introduction

[2] Currently, methane (CH_4) contributes about 20% of the direct anthropogenic radiative forcing by greenhouse gases in the atmosphere [*Shine et al.*, 1995], making it the most important contributor after CO_2 [*Lelieveld et al.*, 1993, 1998]. Owing to various strong methane point sources in the ocean and a possible sink function of this vast environment, the behavior of methane in the ocean is of increasing interest. However, the magnitude of the methane sources and sinks of the marginal and open ocean are still rather uncertain. In this paper, we examine the distribution and biogeochemical behavior of methane in the Weddell Sea and the adjacent Antarctic Circumpolar Current (ACC) using concentration and stable carbon isotope data (Figure 1). In the Southern Ocean, methane has been measured to a limited extent in the Ross Sea [*Lamontagne et al.*, 1974] and Bransfield Strait [*Tilbrook and Karl*, 1994], but no measurements of methane or its carbon isotope ratio have been previously carried out in the Weddell Sea. As in an earlier study in the northern Atlantic [*Rehder et al.*, 1999], the methane data were compared to a data set of the transient tracer chlorofluorocarbon-11 (CCl_3F, referred to as CFC-11 hereinafter) gained on the same expedition. Unlike CH_4, the only source for CFC-11 is air-sea gas exchange and the CFC-11 distribution is entirely controlled by deep-water circulation and mixing [*Weiss et al.*, 1985]. The comparison of CH_4 with CFC-11 combined with the stable carbon isotope ratios of methane permits the determination and quantification of the processes involved in the distribution of methane in an open ocean environment.

[3] There are several potential sources of methane to the deep water of the Weddell Sea. The region is an important source of Antarctic Bottom Water [*Carmack*, 1977; *Foldvik and Gammelsrød*, 1988], and it may be expected that atmospheric methane is transported to the deep ocean, as this is well known for other gases such as oxygen, carbon dioxide (CO_2) [*Weiss et al.*, 1979], and the chlorofluorocarbons (CFCs) [*Foldvik and Gammelsrød*, 1988]. The CFCs have been released in significant amounts into the

[1]GEOMAR Research Center for Marine Geology, Kiel, Germany.
[2]Now at Research Center Ocean Margins, University of Bremen, Bremen, Germany.
[3]Leibniz Institute of Marine Sciences, IFM-GEOMAR, Kiel, Germany.
[4]Institute of Environmental Physics, Bremen, Germany.
[5]Now at Alfred Wegener Institute for Polar and Marine Research, Bremerhaven, Germany.

0886-6236/04/2003GB002151$12.00

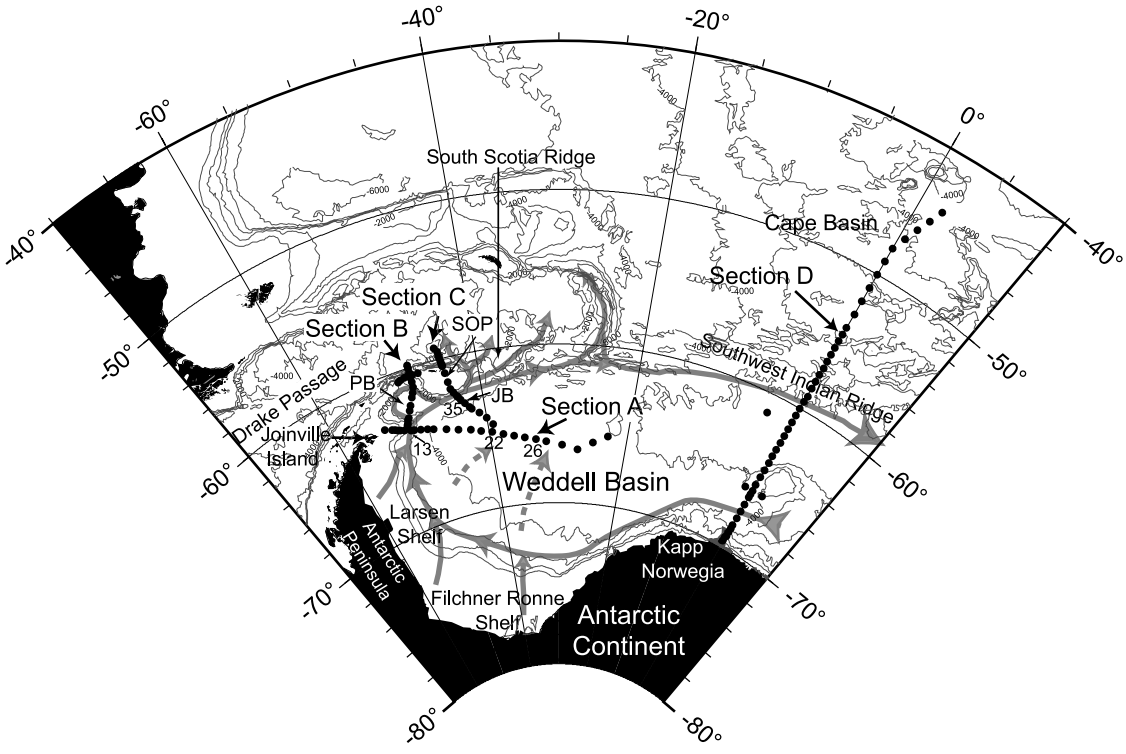

Figure 1. Weddell Sea and adjacent regions, showing CTD stations of the ANT XV/4 cruise that were sampled for methane (dots). Station numbering is indicated next to position for those stations mentioned separately. The shaded lines show the flow of deep water in the Weddell Sea [after *Heywood et al.*, 2002]. PB, Powell Basin; JB, Jane Basin; SOP, South Orkney Plateau.

atmosphere since the late 1950s and have risen monotonically until a maximum was reached in 1996 [*Walker et al.*, 2000]. CFC-11 is inert in seawater on the timescales of at least a few decades and provides a tracer of gas uptake into deep waters formed within recent decades [*Warner and Weiss*, 1985]. In contrast to CFC-11, methane has always been present in the atmosphere, and the most recent increase that began around 1840 has been more gradual (Figure 2).

[4] The potential internal sources of methane to the ocean tend to be local or regional in their nature. These include in situ biological production in the upper water column [e.g., *Tilbrook and Karl*, 1994; *Sansone et al.*, 2001], venting on the sea floor such as hydrothermal systems on mid-ocean ridges [e.g., *Kadko et al.*, 1990; *de Angelis et al.*, 1993; *Charlou et al.*, 1998], cold seeps on continental margins [e.g., *Suess et al.*, 1999; *Valentine et al.*, 2001], and other sediment sources such as generation of methane from buried organic carbon [e.g., *Bernard*, 1979; *Sansone and Martens*, 1981; *Hovland et al.*, 1993]. These sources have no association with CFC-11 and may be detected by anomalously high CH_4/CFC-11 ratios.

[5] The main sink for methane in intermediate and deep waters of the ocean is microbial oxidation. The oxidation rate, R, of methane in seawater appears to be first order with respect to methane concentration [CH_4] [*Ward et al.*, 1987], but the specific oxidation rate, $k_{ox} = R/[CH_4]$, varies widely in different oceanic environments. High specific oxidation rates on the order of 1 to 55 yr^{-1} have been measured in the vicinity of hydrothermal plumes and cold vents, on conti-

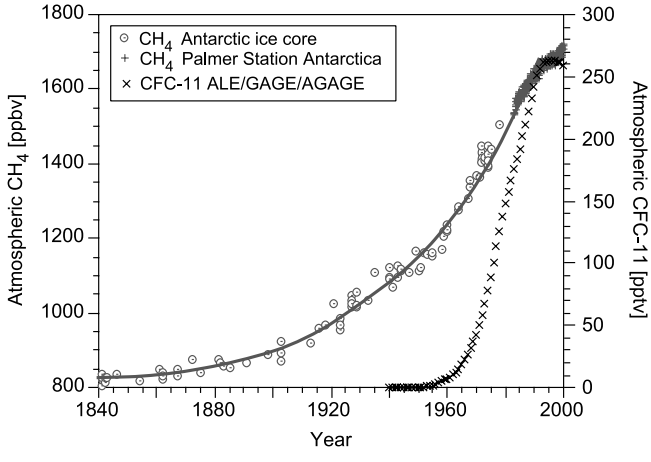

Figure 2. Atmospheric concentrations of CH_4 (circles and crosses) and CFC-11 (stars) over the last 160 years. The CH_4 data of 1841–1979 originate from the Antarctic ice core DE08 [*Etheridge et al.*, 1992] and those from 1980–1998 from Palmer Station (PSA) at 64.92°S and 64°W (*Dlugokencky et al.* [1994] and NOAA cmdl cooperative air sampling network (ftp://ftp.cmdl.noaa.gov/ccg/ch4/flask/)). The CFC-11 data originate from *Prinn et al.* [2000] and the ALE/GAGE/AGAGE network data set (http://cdiac.esd.ornl.gov/ndps/alegage.html).

Table 1. Water Masses of the Western Weddell Sea[a]

Water Mass	Abbreviation	Potential Temperature, °C	Salinity, PSU
Summer Surface Water	AASW	−1.8 to 2.0	33.0–34.3
Winter Water	WW	<−1.7	>34.3
Warm Deep Water	WDW	0 to 0.8	
Modified Warm Deep Water	MWDW	0 to −0.7	34.3–34.64
Weddell Sea Deep Water	WSDW	0 to 0.7	34.64–34.70
Weddell Sea Bottom Water	WSBW	<−0.7	34.60–34.66

[a]After *Foldvik et al.* [1985].

nental shelves, and in particle enriched nepheloid layers [*Sansone and Martens*, 1978; *Kadko et al.*, 1990; *Ward and Kilpatrick*, 1993; *de Angelis et al.*, 1993, 1999; *Tsunogai et al.*, 2000; *Valentine et al.*, 2001]. Methane consumption in newly formed North Atlantic Deep Water appears to proceed more slowly with a specific rate of about 0.02 to 0.1 yr^{-1} [*Scranton and Brewer*, 1978; *Rehder et al.*, 1999]. The corresponding turnover time, $\tau = 1/k_{ox}$, of 10 to 50 years is much shorter than the timescale of the global thermohaline circulation, which is on the order of 500–1000 years [*Broecker and Peng*, 1982]. Thus one would expect methane to be absent in older deep waters. Instead, a relatively constant background concentration of 0.3 to 0.5 nmol L^{-1} persists throughout the deep ocean. Either microbial oxidation ceases below this threshold concentration of methane [*Scranton and Brewer*, 1978] or internal sources such as hydrothermal and cold vents supply sufficient methane to support the background concentration [*Welhan and Craig*, 1983]. It is therefore important to know the size of this sink function for methane of marine and atmospheric sources.

[6] The degree of kinetic isotopic fractionation of carbon isotopes that occurs during methane oxidation in the sea is also uncertain. This fractionation arises because of the preferential use of the isotopically lighter $^{12}CH_4$ by the oxidizing microbes. Thus the rate constant, k_{12}, for the oxidation of $^{12}CH_4$ is slightly greater than k_{13} for $^{13}CH_4$. Laboratory measurements of the fractionation factor, $\alpha = k_{12}/k_{13}$, range from 1.005 to 1.030 [*Zyakun et al.*, 1979; *Barker and Fritz*, 1981; *Coleman et al.*, 1981]. In general, the amount of oxidation estimated from the Rayleigh model is strongly dependent on the fractionation factor used [e.g., *Coleman et al.*, 1981; *Grant and Whiticar*, 2002]. *Tsunogai et al.* [2000] have recently estimated the in situ α to be 1.005 in the water of 4°C inside an undersea caldera that emits hydrothermal methane. Weddell Sea Bottom Water, characterized by potential temperatures below −0.7°C, offers another possibility to investigate isotope fractionation in situ at low temperatures. Such a low fractionation factor would imply that the isotope ratios of methane sources principally determine the distribution of the methane stable carbon isotope ratio ($\delta^{13}C\text{-}CH_4$) in the deep ocean waters and that oxidation has only a minor effect.

[7] It is generally believed that the ocean contributes a small fraction of the total flux of methane to the atmosphere because of oversaturations observed in various continental margin surface waters and in high productivity regions such as the equatorial Pacific. However, previous methane measurements in the Ross Sea and Bransfield Strait showed an undersaturation of CH_4 [*Lamontagne et al.*, 1974; *Tilbrook and Karl*, 1994]. We show here that undersaturation of methane persists in surface waters throughout the Weddell Sea and the Antarctic Circumpolar Current in early fall.

[8] Owing to the local formation of bottom water, the Weddell Sea offers unique opportunities to study the methane oxidation in an open ocean environment. The mean transit time of freshly ventilated Weddell Sea Bottom Water from the surface through the western Weddell Sea to the Greenwich Meridian is on the order of 16 years [*Haine et al.*, 1998; *Klatt et al.*, 2002]. This is comparable to the turnover time of methane in North Atlantic Deep Water [*Scranton and Brewer*, 1978; *Rehder et al.*, 1999]. Methane measurements and sampling for stable carbon isotope measurements were carried out during the ANT XV/4 cruise of the RV *Polarstern* in 1998. The hydrographic sections (Figure 1) intersected the main water masses of the Weddell Sea, including the WSBW at different stages following its formation. In this sampling program a suite of chemical tracers were measured, including the chlorofluorocarbons.

2. Hydrography of the Weddell Sea

[9] For oceanographic investigations, the Weddell Sea is commonly defined as the area enclosed by the cyclonic Weddell Gyre [*Fahrbach and Beckmann*, 2001]. Here we provide a brief overview of the local hydrography because it strongly influences the distribution of the dissolved gases. A detailed review of the circulation is given by *Orsi et al.* [1999]. Hydrographic observations gained on the cruise ANT XV/4 have been presented by *Hoppema et al.* [2001] and *Klatt et al.* [2002]. The water masses referred to in this work are listed in Table 1.

[10] Weddell Sea waters are largely replenished from Lower Circumpolar Deep Water (LCDW), which is diverted from the ACC and enters the Weddell Sea at about 30°E [*Orsi et al.*, 1999]. In the Weddell Gyre it rises to within a few hundred meters of the surface [*Gill*, 1973] and is often referred to as Warm Deep Water (WDW). WDW is practically devoid of anthropogenic tracers such as the CFCs and tritium [*Carmack and Foster*, 1975; *Roether et al.*, 1993; *Orsi et al.*, 1999].

[11] Above the WDW lies the Winter Water (WW), which is a very cold layer of 100–200 m thickness that is formed during winter when the upper mixed layer is convectively overturned at temperatures close to the freezing point [*Gordon and Huber*, 1984]. This layer persists through the summer when it is overlaid by a thin seasonally warmed and relatively fresh layer of Antarctic Surface Water (AASW), which is separated by a shallow pycnocline at about 50 m depth [*Brennecke*, 1921; *Foldvik et al.*, 1985]. Owing to the

entrainment of WDW and the restriction of gas exchange with the atmosphere, the WW and AASW are undersaturated in CFC-11 and, as will be shown, in methane.

[12] In the simplest sense for dissolved gases, Weddell Sea Bottom Water (WSBW) represents end-member mixing of WDW and dense, partially ventilated derivatives of shelf surface waters [*Weiss et al.*, 1979]. These surface waters attain density by brine injection during sea ice formation. Particularly on the Filchner-Rønne and Larsen ice shelves at the southwestern margin of the Weddell Sea, these shelf waters become dense enough to sink. During the subsidence, MWDW (a mixture of WDW and WW) and WDW are entrained. The principal products of this mixing are Weddell Sea Deep Water (WSDW) [*Weppernig et al.*, 1996], in case of the entrainment of a small fraction of shelf water, and WSBW, which includes a higher amount of CFC-11 containing shelf water and is defined by potential temperatures of ≤ -0.7°C [*Carmack and Foster*, 1975; *Foster and Carmack*, 1976; *Foldvik et al.*, 1985; *Fahrbach et al.*, 1995].

[13] The sinking WSDW and WSBW are partly entrained into the boundary current at the northern and western slopes of the Weddell Sea. The uppermost part of this current (<3000 m) exits through various gaps in the South Scotia Ridge after entering the Powell and Jane basins [e.g., *Nowlin and Zenk*, 1988; *Locarnini et al.*, 1993; *Orsi et al.*, 1999; *Gordon et al.*, 2001; *Naveira Garabato et al.*, 2002; *Heywood et al.*, 2002; *Schodlok et al.*, 2002]. The deeper part continues eastward along the slope of the Southwest Indian Ridge to meet the Crozet-Kerguelen Gap at about 55°E [*Reid*, 1989; *Haine et al.*, 1998]. WSBW deposited in a relatively thin layer at the bottom of the Weddell Basin, typically a few hundred meters thick, can reach any of these outlets only after being displaced upward, whereby it enters the overlying Weddell Sea Deep Water regime during recirculation in the basin [*Orsi et al.*, 1993]. The age (time which elapsed since the last contact with the atmosphere) of the freshly ventilated component in the WSBW is therefore higher in the deep basin than it is in the shallower boundary current in the western and northern Weddell Sea.

[14] Weddell Sea Deep Water has traditionally been thought to arise from diffusive mixing of WDW and WSBW. However, recent work indicates that direct production of this deep water mass takes place on the eastern shelves of the Weddell Sea [*Orsi et al.*, 1993; *Fahrbach et al.*, 1995]. In addition, water with WSDW characteristics is transported from the Amery Ice Shelf farther to the east [*Jacobs and Georgi*, 1977; *Klatt et al.*, 2002]. WSDW carries small but significant amounts of CFC-11 [*Klatt et al.*, 2002] and tritium [*Mensch et al.*, 1998].

[15] To the northwest of the Weddell Gyre is a zone of high biological productivity, the Weddell-Scotia Confluence (WSC), which separates the Weddell Sea waters from the Antarctic Circumpolar Current [*Deacon and Foster*, 1977; *Gordon et al.*, 1977; *Gordon*, 1998; *Muench et al.*, 1990; *Orsi et al.*, 1993; *Whitworth et al.*, 1994]. The WSC contains subsided shelf waters originating from the northwestern Weddell Sea and the Bransfield Strait. It extends from the tip of the Antarctic Peninsula eastward as far as the Greenwich Meridian [*Muench et al.*, 1990; *Whitworth et al.*, 1994; *Gordon*, 1998].

3. Methods

[16] Dissolved methane and CFCs were measured on cruise ANT XV/4 aboard RV *Polarstern* (28 March to 23 May 1998) (Figure 1). In addition, we collected samples for the stable carbon signature of methane, while other groups provided temperature, salinity, oxygen, nutrients, CO_2, and helium [*Fahrbach*, 1999].

3.1. CH_4 and CFC-11 Measurements

[17] Dissolved methane was analyzed by the vacuum degassing procedure described by *Rehder et al.* [1999]. Water samples are drawn from the Niskin bottles with glass syringes and then injected into closed evacuated flasks, which are only partially filled. On entering the evacuated flask, the gas and liquid phases separate, with only a small fraction of the gas remaining in the liquid. After shaking for 30 min the gas is transferred and recompressed to atmospheric pressure in a gas burette, from which a 1-mL sample is extracted for methane analysis by gas chromatography. The remaining gas sample is then transferred to an evacuated 5-mL glass bottle sealed with a butyl cap, and these gas samples are returned shoreside for isotopic analysis. The total gas concentration of the sample was determined by adding up the measured dissolved oxygen concentration and the calculated nitrogen and argon concentrations at 100% saturation relative to their atmospheric partial pressures [*Weiss*, 1970]. The dissolved CH_4 concentration was then calculated as the product of the mole fraction in the extracted gas phase and the amount of total gas (STP) in the sample. At CH_4 concentrations of about 0.5 nmol L^{-1} in the central WSDW of section A (n = 44), a standard deviation of ±0.04 nmol L^{-1} was measured. The saturation of CH_4 in the ocean waters was calculated using the methane solubility function given by *Wiesenburg and Guinasso* [1979] and an atmospheric CH_4 concentration of 1.69 ppmv, which was measured at the Palmer Station in April 1998 (ftp://ftp.cmdl.noaa.gov/ccg/ch4/flask/month, cited October 2003).

[18] CFC-11 measurements were carried out using a purge and trap gas chromatographic system with capillary column technique and an electron capture detector. The procedure is described by *Bulsiewicz et al.* [1998]. The precision of these measurements was 1% or 0.004 pmol/kg (whichever is greater). CFC results from ANT XV/4 have been presented and discussed previously by *Hoppema et al.* [2001] and *Klatt et al.* [2002]. In this paper, the apparent saturation of CFC-11 was calculated using the solubility function of *Warner and Weiss* [1985] relative to the 1998 atmospheric mole fraction of 265.5 pptv (ftp://ftp.cmdl.noaa.gov/ccg/cfc/flask/month, cited October 2003).

3.2. Stable Carbon Isotope Measurements

[19] The methane stable carbon isotopic composition was determined with a Continuous Flow Isotope Ratio Mass Spectrometer (CF-IRMS) using a method originally

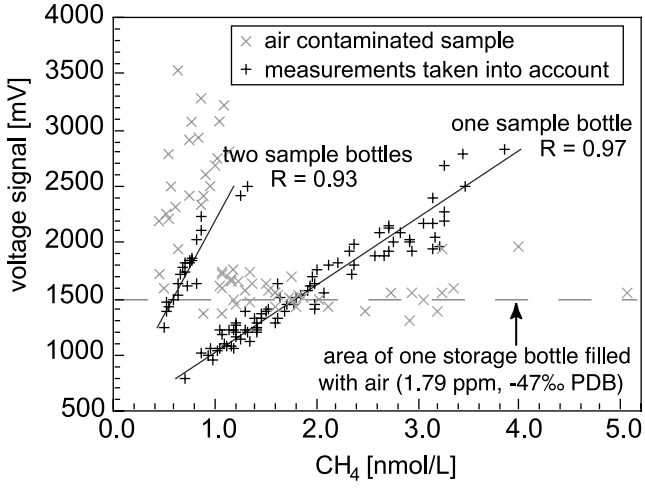

Figure 3. Correlation between the integrated amounts of ions detected in the mass spectrometer (expressed as voltage signal) and the methane concentration for samples of 5 mL gas volume (one storage bottle) and about 10 mL gas volume (two storage bottles). Measurements that deviate from these correlations were contaminated with air during storage (shaded crosses). The degree of the deviation varies depending on the original concentration and the degree of contamination with air in one or two storage bottles.

described by *Merritt et al.* [1995] and modified by *Grant* [2000] at the SEOS laboratory of the University of Victoria. A Finnigan MAT 252 (Finnigan, Bremen, Germany) mass spectrometer was used in combination with a preparative sample pre-concentration loop and a gas chromatograph (GC) linked in series with a combustion reactor (Cu/CuO/Pt at 910°C). After injecting the sample, the contaminants N_2 and O_2 were eluted from a cooled preparative column with a molecular sieve to retain the methane. To increase sensitivity, the open split interface to the CF-IRMS was modified to maximize the amount of sample gas directed into the mass spectrometer [*Grant*, 2000]. Repeatedly measured air samples with voltage amplitudes as low as 500 mV yielded an accuracy of ±0.6‰ PDB (Peedee Belemnite Standard). In order to analyze samples with methane concentrations below 1 nmol L^{-1}, two adjacent gas samples from the same hydrocast with similar methane concentrations (±0.1 nmol L^{-1}) were combined.

[20] A significant fraction of the isotope measurements appear to have been contaminated with air. This probably occurred because the perforation in the butyl cap remaining after the gas sample injection into the storage bottles did not always seal properly. The contaminated samples were sorted out by comparing the original CH_4 concentration and the voltage signal detected by the mass spectrometer (Figure 3). The voltage signal correlates with the CH_4 concentration since the volume of gas sample is constant and the range of the voltage signal is relatively small compared to the total range of the Finnigan MAT 252. A second correlation was observed when two sample volumes were combined for one measurement with the mass spectrometer. A positive excursion in the voltage signal was observed when gas samples with low amounts of methane exchanged with air (1.79 ppmv CH_4), and a negative excursion occurred when high methane samples were contaminated. Complete exchange of sample gas and air during storage produced a voltage signal of about 1500 mV, which equaled the signal of reference bottles filled with air from outside the laboratory. The best data were obtained from sections A and C and are presented in this paper.

3.3. Box Model Simulation

[21] A five-box analog of WSBW formation (Figure 4) was employed to simulate the relationships of methane to CFC-11 and $\delta^{13}C$-CH_4 that appear at differing methane oxidation rates and isotope fractionation factors. For this purpose, a previous three-box model of shelf water formation at 150°E [*Keir et al.*, 1992] was modified to include methane and its carbon isotope ratio. The main feature of the model is the input of a single water source to a vertical two-box shelf domain where finite gas exchange with the surface box takes place. The source water with WDW characteristics enters the shelf domain both directly into the lower box and into the surface box after first being entrained into the off-shelf surface box of the open sea and partially ventilated from the atmosphere. The two shelf boxes exchange water vertically at a finite rate, which is an analog of the convection that takes place during formation of dense shelf waters. In the present model, outflow from the lower shelf box continues through a sequence of two more boxes that represent newly formed (nWSBW) and somewhat older WSBW (oWSBW). WDW also flows into these WSBW boxes to account for entrainment. In the case of methane, this induces a small ''error'' because we observe that the concentration of methane in the WSDW that actually mixes with the deeper WSBW is somewhat lower than in WDW. The tracer concentrations in the source WDW are assumed to be constant over time. In contrast, the mixing ratios of CH_4 and CFC-11 of air exchanging with the surface boxes follow the histories shown in Figure 2. The model simulates the temporal variation of the CFC-11 and CH_4 distributions as forced by these histories.

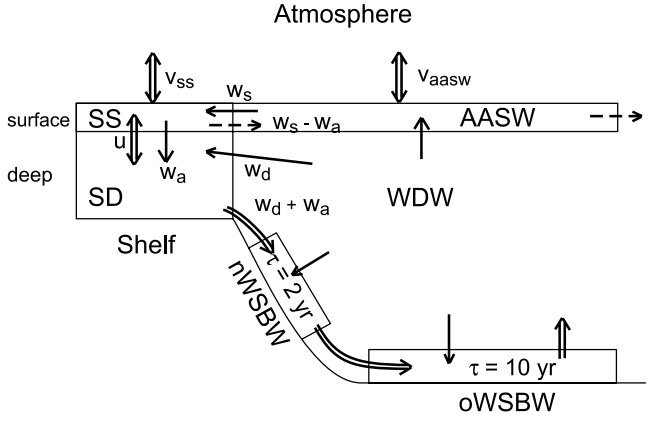

Figure 4. Box model for dissolved gases in Weddell Sea shelf and bottom waters. Dashed arrows indicate transports whose effects are ignored in the model.

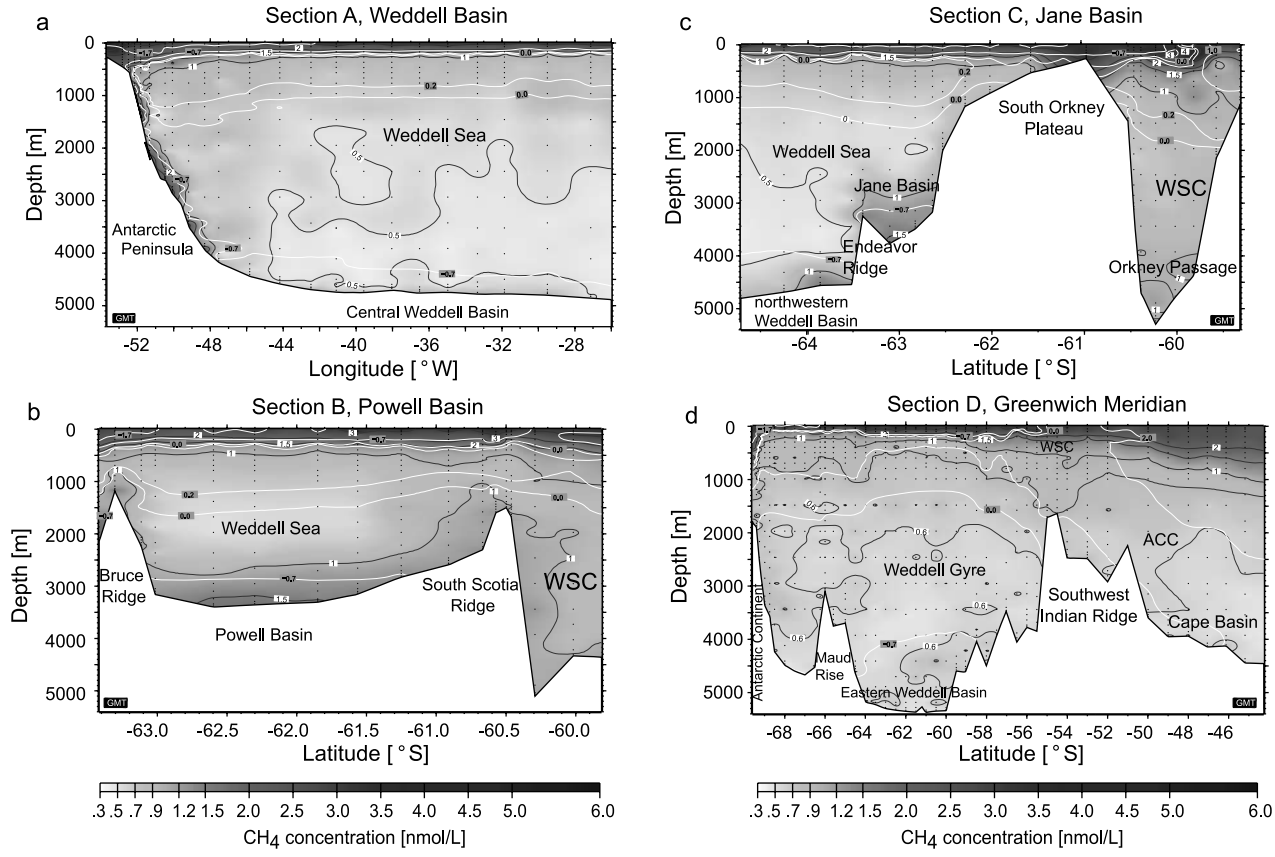

Figure 5. Methane concentrations of four hydrographic sections: (a) along the continental slope of the Antarctic Peninsula and the central Weddell Basin, (b) the Powell Basin and the southern WSC at 48°W, (c) the northwestern Weddell Basin, Jane Basin, South Orkney Shelf, and the WSC at 44°W, and (d) the Weddell Sea, the WSC, and the ACC along the Greenwich Meridian. The white contours show a few major temperature contours (annotation in red; shaded squares in black and white figure), and the black contours show methane concentrations (annotation in black; white boxes in black and white figure). See color version of this figure at back of this issue.

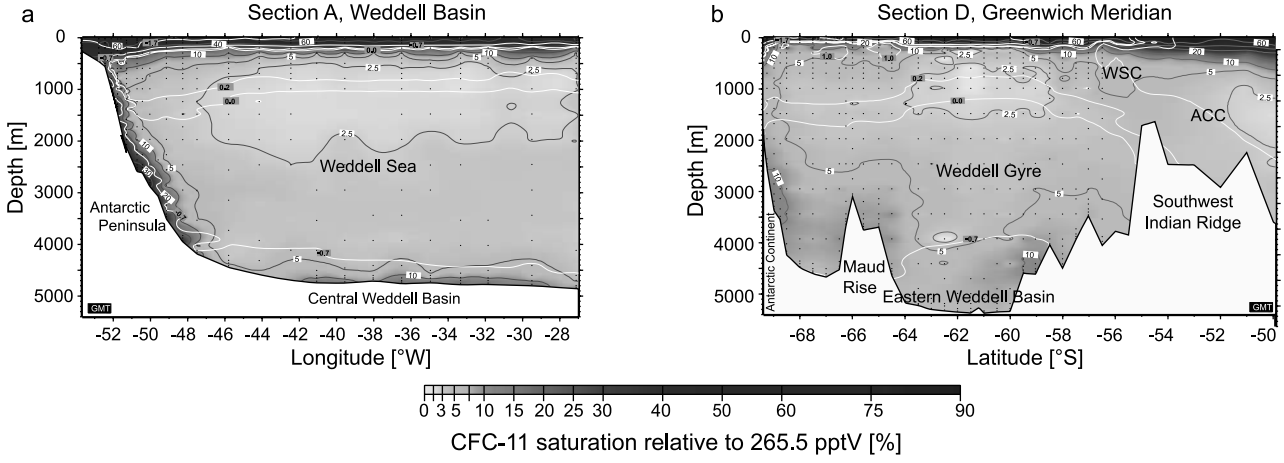

Figure 6. Distribution of dissolved CFC-11, as percentage of saturation with respect to the present atmosphere, along Section A and D [after *Hoppema et al.*, 2001; *Klatt et al.*, 2002]. The white contours show a few major temperature contours (annotation in red; shaded squares in black and white figures), and the black contours show CFC-11 percent saturation (black annotation; white boxes in black and white figure). See color version of this figure at back of this issue.

[22] The rate of methane concentration change in any given box, *i*, is given by the relation

$$h_i \times dc_i/dt = \sum w_j(c_j - c_i) + v_i[c_{Atm}(t) - c_i] - k_{ox}h_ic_i, \quad (1)$$

where h_i is the depth of the box, w_j are the inflows from all adjacent boxes, v_i is the piston velocity for air-sea exchange, $c_{atm}(t)$ is the concentration of the methane at equilibrium with the atmospheric mole fraction at time, t, and k_{ox} is the first-order rate constant for methane oxidation in the box. In order to simulate the time-dependent distribution of the $\delta^{13}C$ of methane, we first note that the product, $q^{13} \equiv \{(1+ \delta^{13}C) \times [CH_4]\}$, is proportional to the concentration of $^{13}CH_4$. The kinetic fractionation factor is conventionally defined as $\alpha = k_{ox}^{12}/k_{ox}^{13}$. Thus q^{13} is simulated by substituting this quantity for $[CH_4]$ and k_{ox}/α for k_{ox} in the equations for methane. After the time integration is complete, $\delta^{13}C$ is back calculated from $\delta^{13}C = q^{13}/[CH_4] - 1$. For the simulation of the stable isotope ratio, we assumed that the $\delta^{13}C$ of atmospheric methane remained constant over time at the present value of −47‰. There appears to be no published record of the atmospheric methane $\delta^{13}C$ over the last century. *Craig et al.* [1986] measured a $\delta^{13}C$ of −49.7‰ in methane extracted from supposedly 300-year-old ice, which indicates that the atmospheric $\delta^{13}C$ has changed very slowly on the average since then. We assume that the methane in WDW enters the model with a $\delta^{13}C$ of −36‰, in accordance with our measurements.

[23] The transport parameters and the individual piston velocities for gas exchange between the surface boxes and the atmosphere were derived from a parameter fit to geochemical data that includes tritium as well as CFC-11. This parameterization sets the timescales of mixing and circulation in the model, which is important to the CH_4-CFC11 relationship that results. In addition, it sets the piston velocity used for the air-sea flux calculations. The procedure we used for the parameterization and the results are described in Appendix A.

4. Results and Discussion

4.1. Distribution of Methane in the Weddell Sea

[24] The distribution of methane in vertical sections across the Weddell Sea is in general similar to that of CFC-11 and thus is related to the distribution and age of the water masses (Figures 5 and 6). The highest CH_4 concentrations are found in the surface layer averaging 3.1 nmol L^{-1}, and these are separated by a strong vertical gradient from the low concentrations found in the bulk of the interior that contains WDW and WSDW. Methane concentrations reach a minimum of 0.4 nmol L^{-1} in WSDW at about 3000 m water depth. At greater depth, a slight increase to 0.6–0.9 nmol L^{-1} is observed in the WSBW at the bottom of the Weddell Basin. Significantly greater concentrations appear on the continental slope and along ridges where recently formed WSBW circulates (Figure 5).

[25] The four hydrographic transects intersect the flow of WSBW as it circulates progressively eastwards on the northern limb of the gyre (Figure 1). The pathway of the WSBW as it leaves the slope of the Antarctic Peninsula, the entrainment of other water masses, and the increasing age as it flows to the east can be traced by the methane concentrations (Figure 5 and Table 2). The CH_4 distribution also mirrors the deviation into a shallower and a deeper limb of the WSBW due to the topography. WSBW at the Antarctic Peninsula has concentrations as high as 2.3 nmol L^{-1} (Figure 5a), and the concentration decreases to a mean of 1.4 nmol L^{-1} in the Powell and Jane basins (Figures 5b and 5c). Part of the WSBW mixes into the overlying WSDW and leaves the Weddell Sea through gaps in the South Scotia Ridge as seen by higher CFC-11 and potential temperatures of −0.6°C in the Orkney Passage. In Section B, elevated methane concentrations up to 1.1 nmol L^{-1} were observed at the bottom of this passage (Figure 5b). The lower limb of WSBW in the boundary current appears at the base of the Endeavor Ridge in the northwestern Weddell Basin (Figure 5c) and contains about 0.9 nmol L^{-1} methane. In section D the WSBW at the deep slope of the Southwest Indian Ridge is hardly noticeable in the methane distribution, since the concentrations are similar compared to those of the surrounding WSDW (Figure 5d).

[26] A comparison of the methane and CFC-11 distributions (Figures 5a, 5d, 6a, and 6b and Table 2) shows that methane decreases concurrently with the CFC-11 as the transit time of WSBW increases. This similarity indicates that air-sea gas exchange is the major source of methane in the Weddell Sea and Antarctic Circumpolar Current. Mixing and convection appear to principally determine the distribution of CH_4 as well as CFC-11 in newly formed bottom water.

4.2. Differences Between the CH_4 and CFC-11 Distributions

[27] Although CFC-11 and methane generally have similar distribution patterns, there are some subtle differences between them. First, in the central Weddell Sea the depth of minimum CH_4 lies deeper in the water column than that of CFC-11 (Figures 5a and 6a). The latter minimum occurs at about 600 m water depth in the core of the WDW coincident with the temperature maximum, but the CH_4 minimum is found between 2000 and 4000 m depth in the WSDW. The minor excess of methane in the shallower water column may be due to methane production in some species of zooplankton [*Cynar and Yayanos*, 1991] and in anoxic microenvironments of sinking particles such as fecal pellets [*Oremland*, 1979; *Sieburth*, 1987; *Marty et al.*, 1997; *de Angelis and Lee*, 1994]. This is a source for methane that is found in the upper 500 m of the ocean elsewhere [*Karl and Tilbrook*, 1994]. However, surface waters of the open Weddell Sea are consistently undersaturated and particle fluxes in the area are low [*Fischer et al.*, 1988]. Besides being produced on site, the excess CH_4 might also originate in the Weddell Scotia Confluence (WSC) and Bransfield Strait, which are zones of higher productivity [e.g., *Whitworth et al.*, 1994; *Fischer et al.*, 2002]. Shallow and intermediate waters from these areas might be introduced into the Weddell Sea.

[28] Another type of difference can be seen along the prime meridian where elevated CFC-11 concentrations exist with no or little methane counterpart (Figures 5d and 6b). At the base of the southern slope of the Southwest Indian

Table 2. Minimum, Maximum, and Average CH_4 and CFC-11 Concentrations and Methane Stable Carbon Isotope Ratios of the WSBW ($T < -0.7°C$) of Various Regions[a]

WSBW Location	Mean CH_4, nmol L^{-1}	Mean SAT, %	Min/Max CH_4, nmol L^{-1}	Min/Max SAT, %	Mean $\delta^{13}C$-CH_4, ‰ PDB	Central $\delta^{13}C$-CH_4, ‰ PDB	Mean CFC-11, pmol/kg	Mean SAT, %	Min/Max CFC-11, pmol/kg	Min/Max SAT, %	Min. Pot. Temp., °C
Antarctic Peninsula	1.85	54	1.20–2.33	35–67	−45.0 ± 0.9 (n = 12)	−45.8	3.109	41	1.70–3.61	23–47	−1.340
Powell Basin	1.42	41	1.19–1.71	35–50	−43.1 ± 0.6 (n = 04)	−43.1	2.204	29	1.80–2.74	24–36	−1.087
Jane Basin	1.37	40	1.24–1.61	37–47	−42.7 ± 0.8 (n = 10)	−43.1	2.056	27	1.77–2.51	24–33	−0.974
Northern Weddell Basin	0.91	27	0.60–1.47	18–43	−42.9 ± 1.9 (n = 03)	−43.9	1.503	20	0.66–2.45	9–32	−1.026
Central Weddell Basin	0.60	18	0.40–0.91	11–27	−41.3 ± 0.5 (n = 05)	−41.5	0.663	9	0.24–1.39	3–19	−0.891
Greenwich Meridian	0.57	17	0.41–0.86	-	-	-	0.539	7	0.31–0.81	4–11	−0.806

[a]SAT, percent saturation relative to the atmospheric mole fraction; Pot. Temp., potential temperature.

Ridge (4500 m depth at 59°S) elevated CFC-11 concentrations show the deep component of WSBW that circulates to the east. However, a methane anomaly is hardly detectable. The same is approximately true at about 3200 m depth adjacent to the Antarctic continental slope on this section. Here an increasing CFC-11 maximum has been detected since 1984, which apparently is due to deep water mass formation on continental shelves somewhere to the east of the prime meridian [*Klatt et al.*, 2002]. This CFC-11 maximum now extends northward from the continental slope to Maud Rise. In the case of CH_4, however, the anomaly is small, and it is confined to the continental slope. This is likely to result from the cumulative oxidation of methane in the CFC-11 containing deep water given enough time after the formation.

[29] A third difference is the higher saturation level of methane found in near-surface waters on partly ice-free inner shelves. This includes the continental shelf (bottom depth: 250–500 m) of the northern Antarctic Peninsula near Joinville Island, where CH_4 saturations up to 166% (5.6 nmol L^{-1}) occur in 40–100 m water depth (Figure 5a). The subsurface maxima on the South Orkney Plateau and in the WSC to the north of the plateau have saturations between 93–152% (Figure 5b). CFC-11 on the other hand was strongly undersaturated below the pycnocline. The origin of the maxima at these two locations, however, might be different as indicated by the stable carbon isotope ratio (see section 4.4).

4.3. CH_4 Versus CFC-11 and Methane Oxidation

[30] With the exception of the oversaturated shelf waters off Joinville Island, a plot of the apparent saturations of CH_4 versus CFC-11 for water masses of the central Weddell Sea shows a general linear correlation (Figure 7a). Close inspection reveals two approximately linear trends separated from each other at low CFC-11 values. The upper trend with a greater methane intercept includes most of the AASW, WW, WDW, the upper part of WSDW, and the WSBW on the slope of the Antarctic Peninsula. The lower trend is observed in deep WSDW and WSBW of the central Weddell Basin.

[31] The plot of CH_4 versus CFC-11 for only the WSBW also shows these two trends, with a discontinuity in the methane values at about 25% CFC-11 saturation (Figure 7b). Besides the recently formed WSBW adjacent to the Antarctic Peninsula, the upper trend at higher CFC-11 is observed in younger WSBW found in the Powell and Jane basins. The lower trend is generally found in older WSBW in the central Weddell Basin, in the deep limb of the boundary current in the northwestern Weddell Basin (Endeavor Ridge) and at the Greenwich Meridian. However, a few samples of WSBW adjacent to the southern slope of the Endeavor Ridge (Figure 7b, crosses) contain apparent CFC-11 saturations greater than 25%, and indeed these are part of the higher methane trend. This indicates that a mixture of boundary current and central basin WSBW is found in the northwestern Weddell Basin. This exchange was also suggested from silicate data by *Hoppema et al.* [1998], who propose that in the northwestern Weddell Sea the injection of water from the margin into the central Weddell Basin may take place.

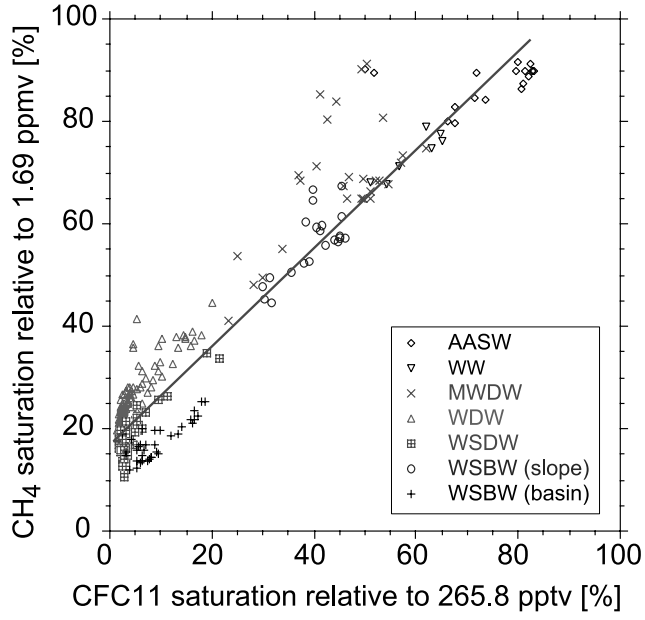

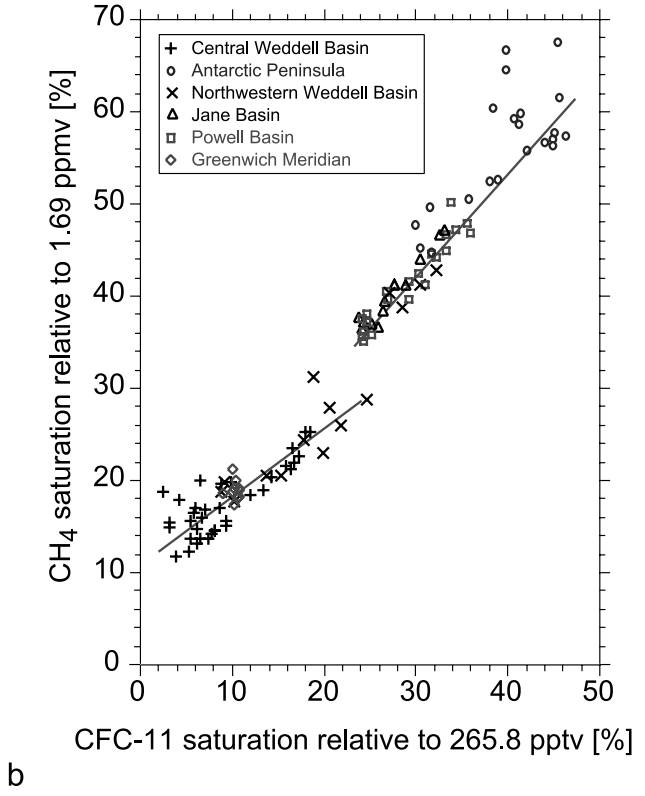

Figure 7. Apparent saturations of CH_4 versus CFC-11 in (a) water masses of the Weddell Basin (Section A), showing a roughly linear correlation between both gases, and (b) Weddell Sea Bottom Water found at various locations as annotated in the box. There is a distinct offset between WSBW with apparent CFC-11 saturations above and below 25%. The seven supersaturated CH_4 values (100–166%) found in the continental shelf waters of the northern Antarctic Peninsula are not plotted.

[32] In subsurface water masses of the western Weddell Sea, the distribution of dissolved oxygen, nitrate, and phosphate appear to be controlled by conservative mixing of dense shelf and warm deep waters [*Weiss et al.*, 1979]. Thus it may be expected that mixing between these end-members will exert an important control on the methane distribution if the mixing occurs rapidly relative to consumption and there are no significant internal sources. If the increases of CFC and methane in the atmosphere also occur on a longer timescale than that of the mixing, it may be expected that these tracers will nearly plot on a mixing line [*Rehder et al.*, 1999].

[33] In addition to mixing and the atmospheric history, the relationship of methane to CFC-11 in WSBW and its precursors will be affected by gas exchange and methane oxidation, as well as the residence time of newly formed bottom water in the Weddell Sea. To consider these effects, time-varying distributions of CFC-11 and methane were simulated in the model shown in Figure 4. A series of methane simulations with different oxidation rate constants were carried out. In these simulations, the rate constant was assumed to be uniform throughout the model and no internal production of methane was assumed to occur. The resulting model-produced CH_4 versus CFC-11 trends for 1998 are plotted in Figure 8a. If no oxidation occurs (k_{ox} = 0), the result is nearly a mixing line between the surface AASW box and the WDW input. As the specific rate of methane oxidation, k_{ox}, increases, CH_4 concentrations decrease below the mixing line, with the largest CH_4 decrease occurring in the old-WSBW box. For any given k_{ox}, the model CH_4 to CFC-11 trend between AASW and old WSBW is still nearly linear. The linearity throughout the WSBW was not observed in the measured data. The observed upper trend of the CH_4-CFC-11 data corresponds to a specific oxidation rate between 0 and 0.02 yr^{-1}, while the observed lower trend corresponds to about 0.06 yr^{-1}. In the former case, the turnover time, τ, of methane ($1/k_{ox}$) is 50 years or greater; in the latter the turnover time is about 17 years.

[34] The model-produced CH_4 versus CFC-11 that results when k_{ox} is 0.02 yr^{-1} everywhere except in old WSBW, where k_{ox} is set at 0.06 yr^{-1}, is shown in Figure 8b. It can be seen that this produces a break in the trend. There would seem to be two possibilities as to why the offset in the methane versus CFC trend occurs. One would be that the specific oxidation rate of methane is higher in WSBW in the central basin than it is in WSBW upstream in the boundary flow. The specific oxidation rate of 0.02 yr^{-1} for the upper trend agrees with the estimate for North Atlantic Deep water using the CH_4 versus CFC-11 trend observed there [*Rehder et al.*, 1999]. It could be that central basin WSBW contains higher concentrations of methane consuming bacteria than are found in the boundary current WSBW, which would promote greater oxidation. However, we have no measurements to support this argument.

[35] The second possible reason for the methane break would be that sources supply methane to shelf precursors of WSBW and/or to newly formed WSBW in the boundary current, but these sources are no longer present in the central basin bottom water. In this case the apparent low specific

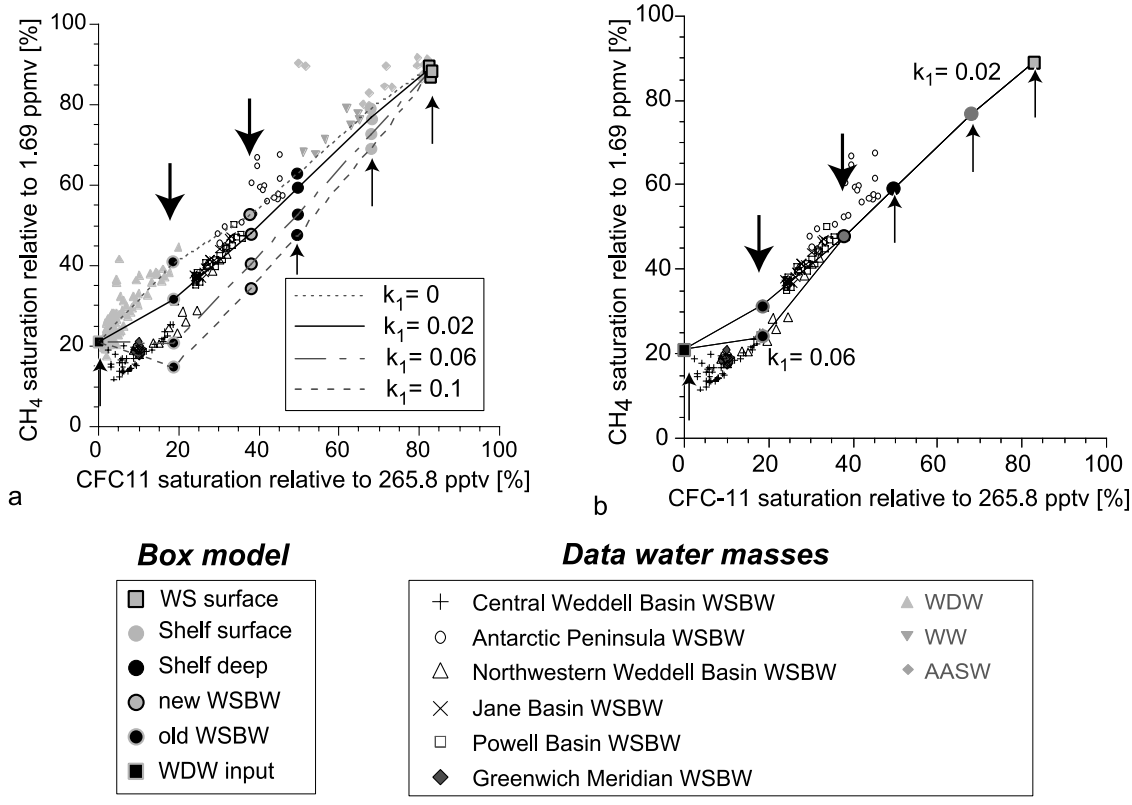

Figure 8. (a) Large points (indicated by arrows) show model-produced CH_4 versus CFC-11 saturation in 1998 for a series of methane specific oxidation rates between 0 and 0.1 yr^{-1}. The boxes of main interest (new WSBW and old WSBW) are marked by bigger arrows. In these simulations, k_{ox} is constant throughout the model. Small points show measured pairs of values for the various water masses. (b) Model-produced CH_4 versus CFC-11 saturation in 1998, when k_{ox} is 0.06 yr^{-1} in old WSBW and 0.02 yr^{-1} elsewhere in the model. Small points show measured data from WSBW at various locations.

rate in the upstream part of the system results from methane input. When this input is no longer present in old WSBW, the true specific oxidation rate is revealed by the methane decrease. The hypothesis of an additional methane source along the slope is supported by positive deviations of methane from the CFC-11 mixing line, which are found in parts of the youngest WSBW on the continental slope of the Antarctic Peninsula (Figures 7a and 7b). These deviations may be due to local emission of methane from the slope sediments, something which has been observed on various continental margins elsewhere [e.g., *Judd et al.*, 2002]. Common isotopic ratios of these methane sources vary between about −35‰ to −60‰. We measured values of about −44‰ PDB in high concentrations of methane (160% saturation) on the shelf near Joinville Island (see Figure 10 in section 4.4). If this is characteristic for sediment sources of methane to the boundary current WSBW, there would be no significant change in the isotopic ratio. Separate formation areas and flow paths of the WSBW may also contribute to the methane discontinuity in this regard. The shallower WSBW is mainly formed under the Larson Ice Shelf [*Fahrbach et al.*, 1995; *Sueltenfuss*, 1998] and transported within the strong boundary current. It appears that the older WSBW in the central Weddell Basin is formed underneath the Filchner-Rønne Ice Shelf and that this descends more directly to the bottom of the Weddell Basin than WSBW in the gyre circulation [*Fahrbach et al.*, 1995]. Thus this component of WSBW may experience less methane input than those WSBW components along slope in the boundary current.

[36] The CH_4 versus CFC-11 in the northern Atlantic shows no obvious indication of methane production in deep water, and *Rehder et al.* [1999] assumed this source to be negligible. However, recent measurements of the methane carbon isotope ratio in this area indicate that the Mid-Atlantic Ridge is a significant source of methane to the water column and that the specific rate of oxidation in the northern Atlantic is closer to 0.06 yr^{-1} [*Keir et al.*, 2003].

[37] This higher specific methane oxidation rate for the open ocean might imply significantly higher sources of methane in the open ocean. The finite background concentration of methane found throughout older water of the deep ocean may mean that oxidation virtually ceases at this level [*Scranton and Brewer*, 1978], or it may be that this is the supported concentration of methane from deep sources. If the latter is true and if the specific oxidation rate deduced in the central Weddell Sea is representative of the normal deep ocean, this would imply that the magnitude of the deep

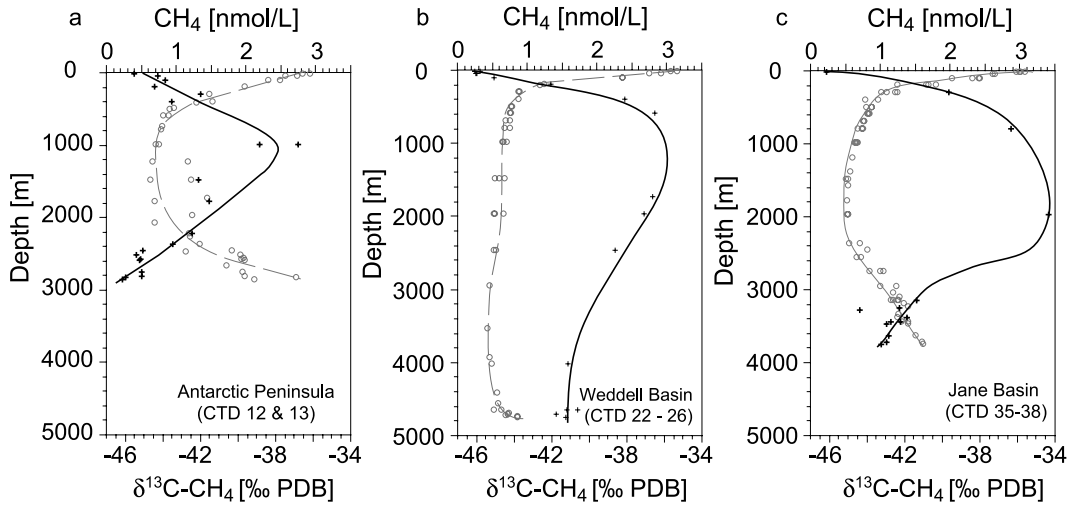

Figure 9. Depth profiles of methane $\delta^{13}C$ at (a) the continental slope of the Antarctic Peninsula, (b) the central Weddell Basin, and (c) the Jane Basin. The shaded open circles mark the corresponding methane concentrations.

source of methane is greater than previously suspected. For example, if the average concentration of 0.3 nmol L^{-1} in 1.3×10^9 km^3 of subsurface water is being oxidized with a specific oxidation rate of 0.02 yr^{-1}, then 8×10^9 mol CH_4 yr^{-1} are being consumed in the deep ocean. If our estimate of 0.06 yr^{-1} for deep WSBW is applicable to the world ocean, the consumption would be three times as great (24×10^9 mol CH_4 yr^{-1}). These consumption rates can be compared to the hydrothermal methane flux of 2.5×10^{-17} mol CH_4 s^{-1} per cm^2 of the Earth's surface [*Welhan and Craig*, 1983], which corresponds to a supply of 4×10^9 mol CH_4 yr^{-1}. This source estimate is based on the CH_4 to ^3He ratio in high temperature vents and presumably represents methane generated by degassing from basalts. If a specific oxidation rate of 0.02 yr^{-1} is normal in the open deep ocean, it would imply that other sources of methane with little associated ^3He provide another 4×10^9 mol CH_4 yr^{-1}. These sources might include cold vents and methane generated by serpentinization, but the magnitude of these sources is not known. If the specific rate of 0.06 yr^{-1} is characteristic of old deep waters, these additional sources would have to provide at least 5 times more methane than the ^3He-associated flux in order to support methane consumption.

4.4. Distribution of $\delta^{13}C$-CH_4 and Isotope Fractionation

[38] The vertical variation of $\delta^{13}C$-CH_4 in the Weddell Sea resembles that of the dissolved methane concentration, with more negative isotopic ratios associated with higher concentrations (Figure 9). The surface water showed $\delta^{13}C$-CH_4 signatures of about −46‰, reflecting the isotope signature of atmospheric methane being dissolved. An influence of isotopically lighter biogenic methane was generally not detected. In association with the decrease in CH_4 in the upper several hundred meters, $\delta^{13}C$-CH_4 increases by about 10‰ and generally reaches a maximum in the WDW at about 1000 m depth. This correlates with the depth of the CFC-11 minimum. In the Jane Basin the maximum in the isotopic ratio is found deeper, at about 2000 m. One thousand meters above the WSBW, $\delta^{13}C$-CH_4 starts to decrease continuously, but the CH_4 concentration increases only slightly until WSBW is encountered near the bottom (Figure 9). In WSBW, the lightest $\delta^{13}C$-CH_4 values are associated with the highest CH_4 concentrations and the lowest temperatures (Table 2). Typical isotopic signatures in WSBW were −45.8‰ PDB along the slope of the Antarctic Peninsula, −43.5‰ PDB in the Powell and Jane basins and south of the Endeavor Ridge, and −41.5‰ PDB in the central Weddell Basin.

[39] When plotted against the reciprocal of methane concentrations, most of the $\delta^{13}C$ measurements lie on a line between surface AASW and the WDW, which are the precursors of all other water masses in the Weddell Basin (Figure 10). This indicates that mixing between these end-members exerts an important control on the distribution of the isotopic ratio.

[40] However, the plot does show a few deviations from the mixing trend. On the South Orkney shelf and north of it, the shallow waters have a strong negative deviation in $\delta^{13}C$-CH_4 that indicates significant in situ production of isotopically light biogenic methane (<−50‰ PDB according to *Whiticar* [1999]). In contrast, the shelf waters near Joinville Island are slightly below the mixing trend with $\delta^{13}C$-CH_4 values of about −44‰ PDB. This may be due to either a small local input of non-biogenic methane (>−50‰ PDB) or to oxidation and isotopic fractionation of a methane pool that was originally lighter.

[41] An interesting deviation from the mixing trend is the lighter than expected $\delta^{13}C$-CH_4 signature of the WSBW in the central Weddell Basin and to some degree in WSDW just above this bottom water. To examine this anomaly, the $\delta^{13}C$ of methane was calculated with the box model for a series of fractionation factors α between 1 and 1.03. Figure 11 is a plot of $\delta^{13}C$-CH_4 ratios versus reciprocal

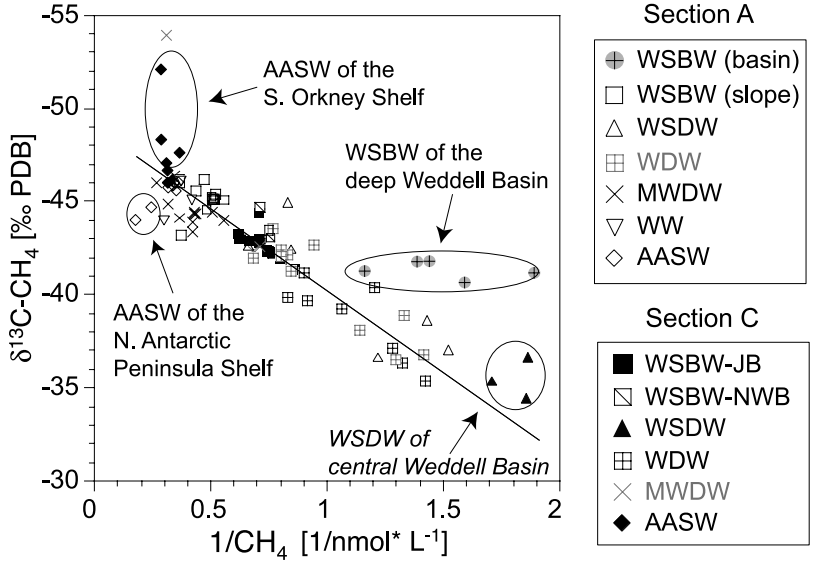

Figure 10. The $\delta^{13}C$ of methane versus the reciprocal of the CH_4 concentration for the water masses of sections A (Weddell Basin) and section C (Jane Basin). Line indicates mixing trend between normal surface waters and Warm Deep Water. JB, Jane Basin; NWB, northwestern Weddell Basin.

methane, when $k_{ox} = 0.02\ yr^{-1}$ throughout the system. One observes that the apparent deviation of $\delta^{13}C$-CH_4 from the mixing line may be either negative or positive, depending on the fractionation factor. Apparent negative deviations occur when the fractionation, i.e., the preferential microbial consumption of $^{12}CH_4$ over $^{13}CH_4$, is low. In this case, oxidation reduces the methane concentration while the isotope ratio remains almost constant. Thus the remaining methane has an isotopically lighter signature than it would have if the reduction in concentration were achieved by mixing with the low concentration, isotopically heavier end-member. Rayleigh fractionation tends to counter this effect as the preferential consumption of $^{12}CH_4$ increases the $\delta^{13}C$ of the remaining methane. From the model results in Figure 11, it appears that an $\alpha > 1.01$ is required to produce positive deviations from the Weddell Sea mixing line.

[42] If there is little isotopic fractionation, the apparent negative deviation of $\delta^{13}C$-CH_4 in WSBW increases with the extent of oxidation. This can be seen by comparing the $\delta^{13}C$ and reciprocal methane concentrations that result in the model when the oxidation rate constant is increased from $0.02\ yr^{-1}$ to $0.06\ yr^{-1}$ in the old-WSBW box (Figure 12). In this example where $\alpha = 1.004$, the effect of the rate increase is to shift the locus to lower concentration (to the right on the diagram) with only a slight increase in $\delta^{13}C$. Thus the apparent deviation of $\delta^{13}C$ from the mixing line becomes more pronounced, which is what we observe in the central basin WSBW. Doubling the residence time of old-WSBW produces an additional decrease in methane concentration with little change in $\delta^{13}C$ (Figure 12).

[43] By comparing Figures 10 and 12, it can be seen that an α of 1.004 produces stable carbon isotope ratios similar to those observed in the WSBW of the central Weddell Basin at temperatures below $-0.7°C$. The finding is in good agreement with results of *Tsunogai et al.* [2000], who estimated the in situ α to be 1.005 in seawater of 4°C within a caldera. In a recent study on the Pacific margin, *Grant and Whiticar* [2002] estimate α to be between 1.002 and 1.013 in waters of the same temperature. Thus it appears that the commonly applied fractionation factor α of 1.025 is too high for natural open oceanic environments. This factor was determined in laboratory experiments with fresh water at temperatures of 26°C [*Coleman et al.*, 1981]. Both the caldera and the Pacific

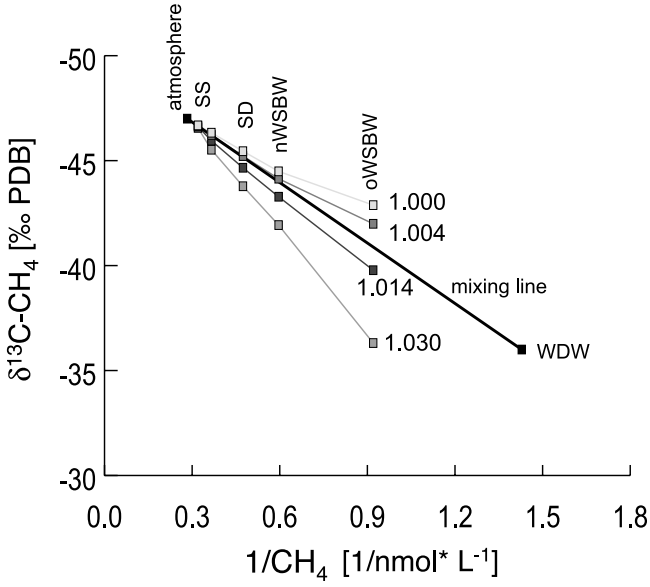

Figure 11. Model-produced $\delta^{13}C$ versus $1/[CH_4]$ in 1998 for a series of fractionation factors α between 1.0 and 1.03. The specific oxidation rate is $0.02\ yr^{-1}$ in all boxes. Pure mixing between WDW and atmospheric end members when no oxidation occurs is shown by the thick line. The surface concentration for the latter is the equilibrium value with the contemporary atmospheric mixing ratio.

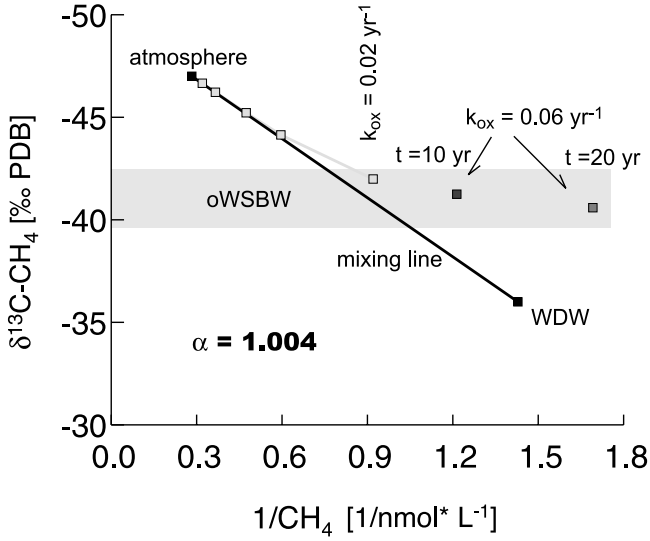

Figure 12. Model-produced $\delta^{13}C$ versus 1/[CH_4] in 1998 where $\alpha = 1.004$ and k_{ox} is 0.02 yr^{-1} in all boxes except for old WSBW. The results of three conditions for old WSBW are shown: (a) where $k_{ox} = 0.02$ yr^{-1} and the residence time of the water (τ) is 10 years, (b) where $k_{ox} = 0.06$ yr^{-1} and $\tau =$ 10 years, and (c) where $k_{ox} = 0.06$ yr^{-1} and $\tau = 20$ years.

margin site are characterized by a wide range of elevated methane concentrations caused by methane venting. Our study in the Weddell Sea shows that low fractionation also occurs in the open ocean containing low methane concentrations. Thus the low fractionation seems to be valid for a wide range of oceanic environments, possibly excluding the shelf areas, where freshwater and riverine input can be important, and the upper tropical ocean, where temperatures are distinctly warmer.

[44] Low isotopic fractionation implies that the $\delta^{13}C$ of methane in the water column mainly reflects the isotopic composition of the sources rather than the effect of Rayleigh fractionation. The application of fractionation factors greater than the true value in Rayleigh models leads to an underestimate of the amount of methane that is oxidized in the ocean. In this way, the primary methane input into the ocean would be underestimated.

4.5. Methane Undersaturation in Surface Waters and Air-Sea Flux

[45] Except for subsurface CH_4 maxima in the WSC and on the outer shelf off Joinville Island, widespread undersaturation of methane and CFC-11 with respect to their present atmospheric mixing ratios was observed in surface waters of the Weddell Sea and the ACC. In the austral autumn the undersaturation of both gases occurs concurrently, and CFC-11 is consistently more undersaturated than methane. The degree of saturation of both gases is roughly correlated to changes in sea surface temperature and decreases to about 80% for CH_4 and 60% for CFC-11 in water near the freezing point. For example, near the continental shelf off of Joinville Island, the degree of saturation of both gases decreases as the surface temperature decreases to the freezing point and the summer pycnocline vanishes (Figure 13). This allows vertical mixing with the residual winter water, which is found below the summer pycnocline and represents the year-old remains of the surface water formed during the former winter. CH_4 and CFC-11 saturations in the winter water were only 75% and 65%, respectively.

[46] The undersaturation of CH_4 and CFC-11 in ice-free, Weddell Sea summer surface water (AASW) averaged about 10% and 20%, respectively. *Tilbrook and Karl* [1994] attributed a similar undersaturation of methane in summer surface waters of the Drake Passage to diapycnal mixing with winter water into the summer layer. In contrast, *Lamontagne et al.* [1974] suggested that methane-utilizing bacteria were responsible for methane undersaturations of up to 20% in a partly ice-covered, calm region of the Ross Sea. From a seasonal model of CFC uptake, *Mensch et al.* [1998] concluded that the time following the retreat of sea ice cover is not sufficient for the 40-m layer of AASW to establish equilibrium with the atmospheric mixing ratio. This appears to be contributed to by the relatively low piston velocity for CFC-11 (336 m yr^{-1}) employed in their model, which is based on a typical wind speed of 5 m s^{-1} for the Weddell Sea and *Wanninkhof*'s [1992] long-term relation. Since this wind speed is only two thirds of the global average, it appears that moderate winds may contribute to the slow equilibration during the period of open water.

[47] The net uptake of CH_4 in the surface water of the Weddell Sea can be estimated from the piston velocity (V_p), the solubility ($\alpha_{CH4} = 0.00209$ nmol L^{-1} ppb^{-1}), and the average atmospheric methane concentration at the Palmer Station in April 1998 ($c_{Atm} = 1694$ ppb). For this calculation, we use the methane piston velocity (400 m yr^{-1}) derived from our box model. The average temperature of the surface water in the Weddell Sea was -1.564°C and the salinity was 34.015. The sea to air flux (F) of CH_4 is given by

$$F = (Sat - 1) \times Vp \times \alpha_{CH4} \times c_{Atm} \times 1000. \quad (2)$$

[48] The average saturation (Sat) of CH_4 in the surface water of the Weddell Sea was 88% (n = 50), which yields

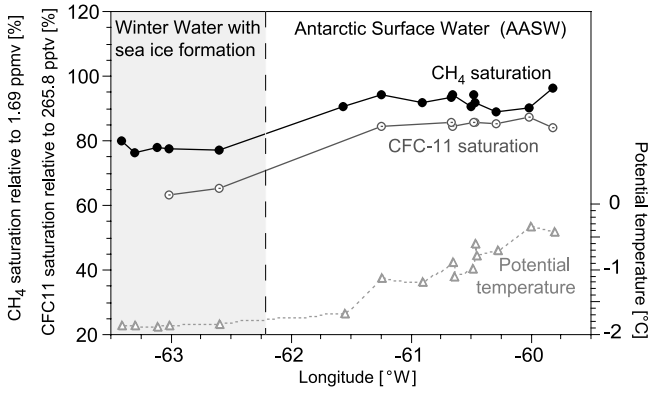

Figure 13. Degree of CH_4 undersaturation versus temperature in the Antarctic Surface Water. The methane saturation parallels the CFC-11 saturation indicating the main influence of air-sea gas exchange for the distribution of CH_4.

a net flux of 0.47 μmol m^{-2} d^{-1} from the atmosphere into the surface water. Methane undersaturation has also been observed in the Drake Passage, where a comparable uptake of CH_4 into the offshore surface waters of 0.35 μmol m^{-2} d^{-1} was estimated [*Tilbrook and Karl*, 1994].

[49] Undersaturation of methane with respect to the atmospheric mole fraction was not restricted to the Weddell Sea; this was also observed throughout the ACC in which an average of about 94% saturation extends as far north as 45°S. Assuming the piston velocity in that region to be somewhere between 600 and 1000 m yr^{-1} due to greater wind speeds as well as less ice coverage, here again one obtains an air-to-sea net flux of about 0.35 to 0.6 μmol m^{-2} d^{-1}. With a sea surface area of 1.8×10^{13} m^2 south of 45°S (excluding all areas shallower than 500 m) and a net flux of 0.5 μmol m^{-2} d^{-1}, we estimate the total uptake of methane in the Southern Ocean to be about 0.05 Tg yr^{-1}. This is small in comparison to the total methane flux of the open ocean to the atmosphere, which was estimated to be between 0.4 to 4.5 Tg yr^{-1} [*Bange et al.*, 1994; *Bates et al.*, 1996]. Estimates of the total marine methane flux including the marginal ocean vary between 18 and 48 Tg yr^{-1} [*Bange et al.*, 1994; *Hornafius et al.*, 1999; *Judd et al.*, 2002].

5. Conclusions

[50] 1. The distribution of methane in the Weddell Sea is mostly controlled by mixing between surface water and old Warm Deep Water during the formation of deep and bottom water. This is indicated by the linear correlations between the apparent CH_4 and CFC-11 saturations and by the mixing trend shown in the comparison of the stable carbon isotopic ratio of methane and the reciprocal of the methane concentration $1/CH_4$.

[51] 2. A significant imprint of methane oxidation in both correlations was observed in the WSBW of the central Weddell Basin. Model simulations suggest a value of the specific oxidation rate of 0.06 yr^{-1} in this water mass, which likely applies for the overall bottom water in the Weddell Sea. This equals a turnover time of 17 years.

[52] 3. The related carbon isotope ratios of methane indicate that the kinetic fractionation for methane oxidation in the bottom water is low ($\alpha = 1.004$).

[53] 4. Warm Deep Water has slightly greater methane concentrations than found at depth in the Weddell Sea Deep Water, which is in contrast to the distribution of CFC-11. This is likely due to a low rate of in situ methane production within WDW or might originate in transport of methane from high productivity zones, namely the Weddell Scotia Confluence and the Bransfield Strait.

[54] 5. In tandem with CFC-11, the surface waters of the Weddell Sea and the ACC were generally undersaturated in CH_4 by 6–25% with respect to the present atmospheric mole fraction. From the model-deduced piston velocities, an air to sea flux of methane of about 0.5 μmol m^{-2} d^{-1} was estimated, which yields a total net uptake of 0.05 Tg CH_4 yr^{-1} for the entire Southern Ocean. This uptake of CH_4 is small in the face of the total methane source term of the ocean.

Appendix A: Box Model of Gas Tracers in WSBW Formation: Physical Parameters

[55] For the purpose of calibrating the physical parameters in the model, CFC-11, tritium, and radiocarbon were also simulated with the model. Equations for these tracers and a discussion of how they constrain the model parameters are presented by *Keir et al.* [1992]. In the case of tritium, the observed history of tritium in off-shelf Weddell Sea surface waters [*Bayer and Schlosser*, 1991] was prescribed as the horizontal concentration input to the on-shelf surface box. We assume that this surface water also receives tritium deposition and that this flux is equal to the deposition to the off-shelf Weddell Sea surface. This assumption may not strictly be true because of the more southerly location of the shelf, transport of sea ice, etc., but this serves as a first approximation. The deposition flux of tritium to the shelf surface water is derived from the off-shelf concentration function and the rate of WDW input to the off-shelf Weddell Sea surface waters as described by *Mensch et al.* [1998].

[56] The physical parameters in the model (Figure 4) were assigned according to the following considerations. It is assumed that upward transport of WDW is the only supply of water to the off-shelf AASW box, and horizontal transports to this box, whether from the continental shelf areas or from the north, are ignored. For such systems, entrainment rates of 30 to 60 m yr^{-1} have been derived from various tritium models [*Michel*, 1978, 1984; *Weiss et al.*, 1979; *Mensch et al.*, 1998]. This input regulates the other transport parameters in the model, for example, the piston velocities for gas exchange. We employed 60 m yr^{-1} for the entrainment rate, as this gives an upper limit to what the model gas exchange rates can be. As discussed below, these are still significantly lower than expected for open ocean waters.

[57] The piston velocities for gas exchange with the AASW box were then adjusted until a reasonable match to our observations in open Weddell surface waters was found. We assumed the ratio of CH_4 to CFC-11 piston velocities to be fixed at 1.4 because at normal wind velocities the piston velocity is predicted to be inversely proportional to the square root of the Schmidt number [*Wanninkhof*, 1992]. At 0°C, the Schmidt number for CFC-11 is about twice that of methane. Piston velocities of 285 m yr^{-1} for CFC-11 and 399 m yr^{-1} for methane produce AASW concentrations in 1998 that are close to those observed. The piston velocity for CO_2 is expected to be about the same as that for methane because the Schmidt numbers of these two gases are similar in cold water. The value of 399 m yr^{-1} is about one third of the piston velocity that would be expected for CO_2 from the global average exchange flux of 22 mol m^2 yr^{-1}. This reduction may be due to restriction by sea ice coverage that varies seasonally in the open Weddell Sea [*Weiss et al.*, 1979]. However, this value of the CO_2 piston velocity is about half the value derived from the simulation of radiocarbon uptake in the Weddell Sea surface using the same entrainment of

Table A1. Shelf Parameters in the Model[a]

Case	w_d	u	w_s	w_a	v_{ss}(F11)	$v_{ss}(CH_4)$
No down advection	76	211	72	0	94	132
Complete down advection	98	182	71	71	82	115

[a]All transports are given in the equivalent of vertical velocity, in m yr^{-1}.

60 m yr^{-1} [*Michel and Linick*, 1985]. (The AASW portion of our model is the same as theirs and gives the same ^{14}C result with identical piston velocities.) The discrepancy may arise because horizontal transport of surface water into the Weddell Sea from the north is ignored in these models. The radiocarbon level in shelf surface water is much more sensitive to horizontal transport than the CFC and tritium concentrations [*Keir et al.*, 1992], and *Michel and Linick*'s [1985] measurements show that greater surface values of $\Delta^{14}C$ existed in the adjacent Scotia Sea than in the Weddell Sea during 1981. Thus inflow from the Scotia Sea may have supported a somewhat higher level of surface radiocarbon in the Weddell surface than otherwise would have existed.

[58] Inputs of AASW and WDW, vertical mixing rate, net downward advection, and air-sea gas exchange control the tracer concentrations in the shelf boxes. We constrained these parameters to produce (1) a value of 200 mTU (1 TU $\equiv$ [T]/[H] = 10^{-18}) for tritium in the upper shelf box in 1987 and (2) the CFC-11 and methane concentrations we observed in the cold surface waters close to the continental shelf in 1998. The tritium concentration is approximately that measured by *Bayer and Schlosser* [1991] in surface waters over the sill separating the Filchner Depression from the Weddell Sea. In addition, the model was constrained to produce a CFC-11 value of about 3.5 pmol kg^{-1} in the lower shelf box in 1992. This is based on the measurements of *Gammelsrød et al.* [1994] in front of the Rønne and Filchner ice shelves. The distribution of the CFCs below the halocline was much more inhomogeneous than that of dissolved oxygen, which varies between 310 to 320 μmol kg^{-1}. Our target value for CFC-11 is a visually estimated average from the sections of *Gammelsrød et al.* [1994].

[59] By trial and error, we obtained two parameter sets that achieve the targeted tracer values in the shelf boxes (Table A1). The set of parameters needed to satisfy a multitracer distribution in the two-box shelf is non-unique [*Keir et al.*, 1992], and one must assign what fraction of the horizontal inflow to the shelf surface box exits horizontally at the surface and what fraction exits from the lower box. The parameter sets in Table A1 bracket the range of 100% outflow at the surface with no net downward advection ($w_a = 0$) to 100% sinking of the inflow ($w_a = w_s$) with no net outflow at the surface. The piston velocities of a particular gas for the shelf surface water derived from either of these extremes differ by only about 10%.

[60] The piston velocities of CFC-11 and methane for the shelf surface water (Table A1) are considerably lower than even the piston velocities derived for the open Weddell Sea surface water. The value of about 120 m yr^{-1} for methane is about a factor of 10 lower than expected from the global CO_2 exchange flux in cold water. The shelf waters have extensive sea ice coverage throughout the year, and therefore such a reduction in air-sea exchange rate may be reasonable. The total input of surface water and WDW to the shelf boxes, $w_s + w_d$, obtained from either set of parameters is not very different; the residence time of this input to the combined surface and sub-surface volume of the shelf is 3.6 to 4 years. However, the outflow from the lower shelf box (analogous to WSBW formation), $w_d + w_a$, varies by a factor of 2 between the two cases in Table A1. In regard to CFC-11 and methane downstream in the WSBW boxes, it does not matter which one of the parameter sets in Table A1 is chosen because (1) they both produce identical histories of these tracers in the shelf boxes (Figure A1) and

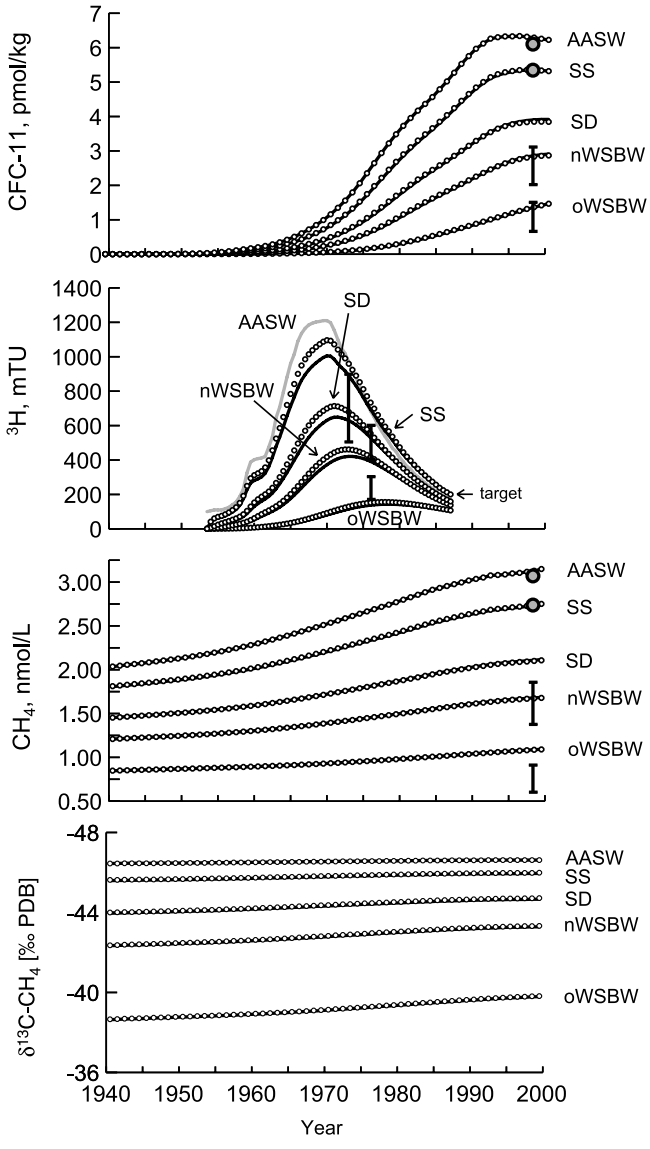

Figure A1. Model output resulting from the physical parameters in Table A1. Lines show result when no net downward advection on shelf occurs; small points show the case where all on shelf surface transport is converted to overflow. Points show target values of the model simulation. See Figure 4 for box labeling.

(2) the tracer equations for the WSBW boxes are parameterized in terms of the water residence times.

[61] The overflow from the shelf mixes with the WDW source in the two WSBW boxes. We fixed the proportions of entrained WDW based on potential temperatures observed in these water masses. In the first WSBW box representing "newly formed" WSBW, the mixture consists of three parts shelf water to one part WDW. Two parts of this new WSBW then mix with one part of WDW to become "old" WSBW in the second box. Thus, in the second WSBW box, the ratio of lower shelf box water to WDW is one to one. We assume that the residence time of the total input to the new-WSBW box is 2 years. The WSBW of the Jane Basin was determined by *Schlosser et al.* [1991] to be less than 5 years old. In most cases we assume that the residence time of the combined input of new-WSBW and WDW to the second WSBW box is 10 years. Most recent dating of the WSBW in the boundary current at the Greenwich Meridian by CFC-11 resulted in an age of 12–14 years [*Klatt et al.*, 2002; *Haine et al.*, 1998]. These residence times are also similar to those estimated by *Michel* [1978] based on his measurements of tritium in these water masses in 1975. An example of the model-produced histories of CFC-11, methane, its $\delta^{13}C$ and tritium simulated by the model are shown in Figure A1. In the case of methane, two additional parameters must be specified - the oxidation rate constant and isotope fractionation factor. For the example in Figure A1, these are set at 0.02 yr^{-1} and 1.014. For the most part, it appears that the simulated tritium and CFC histories correspond reasonably well with historical observations.

[62] **Acknowledgments.** We greatly appreciate the support at sea by the masters and crews of R/V *Polarstern* and our thanks goes to E. Fahrbach, who enabled our participation on the cruise. We also thank Karin Fürhaupter for her really indispensable help at sea. We thank D. L. Valentine and an unknown reviewer for their very helpful comments on the manuscript. Financial support for this work was granted by the Deutsche Forschungsgemeinschaft (SU 114/6-1 to SU 114/6-3).

References

Bange, H. W., U. H. Bartell, S. Rapsomanikis, and M. O. Andreae (1994), Methane in the Baltic and North Seas and a reassessment of the marine emissions of methane, *Global Biogeochem. Cycles*, *8*, 465–480.

Barker, J. F., and P. Fritz (1981), Carbon isotope fractionation during microbial methane oxidation, *Nature*, *293*, 289–291.

Bates, T. S., K. C. Kelly, J. E. Johnson, and R. H. Gammon (1996), A reevaluation of the open ocean source of methane to the atmosphere, *J. Geophys. Res.*, *101*(D3), 6953–6961.

Bayer, R., and P. Schlosser (1991), Tritium profiles in the Weddell Sea, *Mar. Chem.*, *35*, 123–136.

Bernard, B. B. (1979), Methane in marine sediments, *Deep Sea Res., Part A*, *26*, 429–443.

Brennecke, W. (1921), Die ozeanographischen Arbeiten der deutschen Antarktischen Expedition 1911–1912, *Arch. Dtsch. Seewarte*, *39*, 214 pp.

Broecker, W. S., and T. H. Peng (1982), *Tracers in the Sea*, 690 pp., Lamont-Doherty Geol. Observ., Columbia Univ., New York.

Bulsiewicz, K., H. Rose, O. Klatt, A. Putzka, and W. Roether (1998), A capillary-column chromatographic system for efficient chlorofluorocarbon measurement in ocean waters, *J. Geophys. Res.*, *103*(C8), 15,959–15,970.

Carmack, E. D. (1977), Water characteristic of the Southern Ocean south of the Polar Front, in: *A Voyage of Discovery: George Deacon 70th Anniversary Volume*, edited by M. Angel, pp. 15–43, Pergamon Press, New York.

Carmack, E. D., and T. D. Foster (1975), On the flow of water out of the Weddell Sea, *Deep Sea Res.*, *22*, 711–724.

Charlou, J. L., Y. Fouquet, H. Bougault, J. P. Bonval, J. Etoubleau, P. Jean-Baptiste, A. Dapoigny, P. Appriou, and P. A. Rona (1998), Intense CH4 plumes generated by serpentinisation of ultramafic rocks at the intersection of the 15°20′N fracture zone and the Mid-Atlantic Ridge, *Geochim. Cosmochim. Acta*, *62*, 2323–2333.

Coleman, D. D., J. B. Risatti, and M. Schoell (1981), Fractionation of carbon and hydrogen isotopes by methane-oxidizing bacteria, *Geochim. Cosmochim. Acta*, *45*, 1033–1037.

Craig, H., C. C. Chou, C. M. Stevens, and A. Engelkemeir (1986), Isotopic composition of carbon and methane from polar ice cores, *Eos Trans. AGU*, *67*, 245.

Cynar, F. J., and A. A. Yayanos (1991), Enrichment and characterization of a methanogenic bacterium from the oxic layer of the ocean, *Curr. Microbiol.*, *23*, 89–96.

Deacon, G. E. R., and T. D. Foster (1977), The boundary region between the Weddell Sea and Drake Passage currents, *Deep Sea Res.*, *24*, 505–510.

de Angelis, M. A., and C. Lee (1994), Methane production during zooplankton grazing on marine phytoplankton, *Limnol. Oceanogr.*, *39*, 1298–1308.

de Angelis, M. A., M. D. Lilley, E. J. Olson, and J. A. Baross (1993), Methane oxidation in deep-sea hydrothermal plumes of the Endeavor segment of the Juan de Fuca Ridge, *Deep Sea Res., Part I*, *40*, 1169–1186.

de Angelis, M. A., R. W. Collier, G. Klinkhammer, M. E. Torres, and K. Heeschen (1999), Oxidation of methane derived from gas hydrates of the Cascadia accretionary prism, *Eos Trans. AGU*, *80*(46), Fall Meet. Suppl., F635.

Dlugokencky, E. J., L. P. Steele, P. M. Lang, and K. A. Masarie (1994), The growth rate and distribution of atmospheric methane, *J. Geophys. Res.*, *99*(D8), 17,021–17,043.

Etheridge, D. M., G. I. Pearman, and P. J. Fraser (1992), Changes in tropospheric methane between 1841 and 1978 from a high accumulation-rate Antarctic ice core, *Tellus, Ser. B*, *44*, 282–294.

Fahrbach, E. E. (1999), Die Expedition ANTARKTIS XV/4 des Forschungsschiffes *'Polarstern'* 1998/The expedition ANTARKTIS XV/4 of the research vessel *'Polarstern'* in 1998, in *Ber. Polarforsch.*, *314*, 109 pp.

Fahrbach, E., and A. Beckmann (2001), Weddell Sea Circulation, in *Encyclopedia of Ocean Sciences*, edited by J. H. Steele and K. K. Tureltian, pp. 3201–3208, Academic, San Diego.

Fahrbach, E., G. Rohardt, M. Schröder, V. Strass, and A. Wisotzki (1995), Formation and discharge at deep and bottom water in the northwestern Weddell Sea, *J. Mar. Res.*, *53*, 515–538.

Fischer, G., B. Fütterer, R. Gersonde, S. Honjo, D. Ostermann, and G. Wefer (1988), Seasonal variability of particle flux in the Weddell Sea and its relation to ice cover, *Nature*, *335*, 426–428.

Fischer, G., R. Gersonde, and G. Wefer (2002), Organic carbon, biogenic silica and diatom fluxes in the marginal winter sea-ice zone and in the Polar Front Region: Interannual variations and differences in composition, *Deep Sea Res., Part II*, *49*, 1721–1745.

Foldvik, A., and T. Gammelsrød (1988), Notes on Southern Ocean hydrography, sea-ice and bottom water formation, *Palaeogeogr. Palaeoclimatol. Palaeoecol.*, *67*, 3–17.

Foldvik, A., T. Gammelsrød, and T. Toressen (1985), Circulation and water masses on the southern Weddell Sea shelf, in *Oceanology of the Antarctic Continental Shelf*, *Antarct. Res. Ser.*, vol. 43, edited by S. S. Jacobs, pp. 5–20, AGU, Washington, D. C.

Foster, T. D., and E. D. Carmack (1976), Frontal zone mixing and Antarctic Bottom Water formation in the southern Weddell Sea, *Deep Sea Res.*, *23*, 301–317.

Gammelsrød, T., A. Foldvik, O. A. Nøst, Ø. Skagseth, L. G. Anderson, E. Fogelqvist, K. Olsson, T. Tanhua, E. P. Jones, and S. Østerhus (1994), Distribution of water masses on the continental shelf in the southern Weddell Sea, in *The Polar Oceans and Their Role in Shaping the Global Environment*, *Geophys. Monogr. Ser.*, vol. 84, edited by O. M. Johannessen, R. D. Muench, and J. E. Overland, pp. 159–176, AGU, Washington D. C.

Gill, A. E. (1973), Circulation and bottom water production in the Weddell Sea, *Deep Sea Res.*, *20*, 111–140.

Gordon, A. L. (1998), Western Weddell Sea thermohaline stratification, in *Ocean, Ice, and Atmosphere*, *Antarctic Res. Ser.*, vol. 75, edited by S. S. Jacobs and R. F. Weiss, pp. 215–240, AGU, Washington D. C.

Gordon, A. L., and B. A. Huber (1984), Thermohaline stratification below the Southern Ocean sea ice, *J. Geophys. Res.*, *89*, 641–648.

Gordon, A. L., D. T. Georgi, and H. W. Taylor (1977), Antarctic polar front zone in the western Scotia Sea-Summer 1975, *J. Phys. Oceanogr.*, *7*, 309–328.

Gordon, A. L., M. Visbeck, and B. Huber (2001), Export of Weddell Sea Deep and Bottom Water, *J. Geophys. Res.*, *106*, 9005–9017.

Grant, N. J. (2000), Stable carbon isotopic evidence for bacterial oxidation and mixing in two deep-sea methane plumes, Master of Sci., 188 pp., Univ. of Victoria, Victoria, B. C., Canada.

Grant, N. J., and M. J. Whiticar (2002), Stable carbon isotopic evidence for methane oxidation in plumes above Hydrate Ridge, Cascadia Oregon Margin, *Global Biogeochem. Cycles*, *16*(4), 1124, doi:10.1029/2001GB001851.

Haine, T. W. N., A. J. Watson, M. I. Liddicoat, and R. R. Dickson (1998), The flow of Antarctic Bottom Water to the southwest Indian Ocean estimated using CFCs, *J. Geophys. Res.*, *103*(C12), 27,637–27,653.

Heywood, K. J., A. C. Naveira Garabato, and D. P. Stevens (2002), High mixing rates in the abyssal Southern Ocean, *Nature*, *415*, 1011–1014.

Hoppema, M., E. Fahrbach, K. U. Richter, H. J. W. de Baar, and G. Kattner (1998), Enrichment of silicate and CO_2 and circulation of the bottom water in the Weddell Sea, *Deep Sea Res., Part I*, *45*, 1797–1817.

Hoppema, M., O. Klatt, W. Roether, E. Fahrbach, K. Bulsiewicz, C. Rodehacke, and G. Rohardt (2001), Prominent renewal of Weddell Sea Deep Water from a remote source, *J. Mar. Res.*, *59*, 257–279.

Hornafius, J. S., D. Quigley, and B. P. Luyendyk (1999), The world's most spectacular marine hydrocarbon seeps (Coal Oil Point, Santa Barbara Channel California): Quantification of emission, *J. Geophys. Res.*, *104*(C9), 20,703–20,711.

Hovland, M., A. G. Judd, and R. A. J. Burke (1993), The global flux of methane from shallow submarine sediments, *Chemosphere*, *26*(1–4), 559–578.

Jacobs, S. S., and D. T. Georgi (1977), Observations on the southwest Indian/Antarctic Ocean, in *Voyage of Discovery*, edited by M. Angel, pp. 43–85, Pergamon, New York.

Judd, A. G., M. Hovland, L. I. Dimitrov, S. García Gil, and V. Jukes (2002), The geological methane budget at continental margins and its influence on climate change, *Geofluids*, *2*, 109–126.

Kadko, D. C., N. D. Rosenberg, J. E. Lupton, W. R. Collier, and M. D. Lilley (1990), Chemical reaction rates and entrainment within the Endeavor Ridge hydrothermal plume, *Earth Planet. Sci. Lett.*, *99*, 315–335.

Karl, D. M., and B. D. Tilbrook (1994), Production and transport of methane in oceanic particulate organic matter, *Nature*, *368*, 732–734.

Keir, R. S., R. L. Michel, and R. F. Weiss (1992), Ocean mixing versus gas exchange in Antarctic Shelf Waters near 150°E, *Deep Sea Res.*, *39*, 97–119.

Keir, R. S., J. Greinert, G. Petrick, M. Rhein, and D. Wallace (2003), Methane emission from the Mid-Atlantic Ridge near the Gibbs Fracture Zone, *Geophys. Res. Abstr.*, *5*, 05750.

Klatt, O., W. Roehter, M. Hoppema, K. Bulsiewicz, U. Fleischmann, C. Rodehacke, E. Fahrbach, R. F. Weiss, and J. L. Bullister (2002), Repeated CFC sections at the Greenwich Meridian in the Weddell Sea, *J. Geophys. Res.*, *107*(C4), 3030, doi:10.1029/2000JC000731.

Lamontagne, R. A., J. W. Swinnerton, V. J. Linnenbom, and W. D. Smith (1974), C_1–C_4 hydrocarbons in the North and South Pacific, *Tellus*, *26*, 71–77.

Lelieveld, J., P. J. Crutzen, and C. Brühl (1993), Climate effects of atmospheric methane, *Chemosphere*, *26*, 739–768.

Lelieveld, J., P. J. Crutzen, and F. J. Dentener (1998), Changing concentration, lifetime and climate forcing of atmospheric methane, *Tellus, Ser. B*, *50*, 128–150.

Locarnini, R. A., T. Whitworth III, and W. D. Nowlin Jr. (1993), The importance of the Scotia Sea on the outflow of Weddell Sea Deep Water, *J. Mar. Res.*, *51*, 135–153.

Marty, D., P. Nival, and W. D. Yoon (1997), Methanoarchaea associated with sinking particles and zooplankton collected in the northeastern tropical Atlantic, *Oceanol. Acta*, *20*, 863–869.

Mensch, M., A. Simon, and R. Bayer (1998), Tritium and CFC input functions from the Weddell Sea, *J. Geophys. Res.*, *103*(C8), 15,923–15,937.

Merritt, D. A., J. M. Hayes, and D. J. Des Marais (1995), Carbon isotopic analysis of atmospheric methane by isotope-ratio-monitoring gas chromatography-mass spectrometry, *J. Geophys. Res.*, *100*(D1), 1317–1326.

Michel, R. L. (1978), Tritium distribution in Weddell Sea water masses, *J. Geophys. Res.*, *83*(C12), 6192–6198.

Michel, R. L. (1984), Oceanographic structure of the eastern Scotia Sea: 2. Chemical oceanography, *Deep Sea Res.*, *31*, 1157–1168.

Michel, R. L., and T. W. Linick (1985), Uptake of bomb-produced carbon-14 by the Weddell Sea, *Meteoritics*, *20*, 423–435.

Muench, R. D., J. T. Gunn, and D. M. Husby (1990), The Weddell-Scotia Confluence in midwinter, *J. Geophys. Res.*, *95*(C10), 18,503–18,515.

Naveira Garabato, A. C., K. J. Heywood, and D. P. Stevens (2002), Modification and pathways of Southern Ocean Deep Waters in the Scotia Sea, *Deep Sea Res., Part I*, *49*, 681–705.

Nowlin, W. D., Jr., and W. Zenk (1988), Westward bottom currents along the margin of the south Shetland island arc, *Deep Sea Res.*, *35*, 269–301.

Oremland, R. S. (1979), Methanogenic activity in plankton samples and fish intestines: A mechanism for in situ methanogenesis in oceanic surface waters, *Limnol. Oceanogr.*, *24*(6), 1136–1141.

Orsi, A. H., W. D. Nowlin Jr., and T. Whitworth III (1993), On the circulation and stratification of the Weddell Gyre, *Deep Sea Res., Part I*, *40*, 169–203.

Orsi, A. H., G. C. Johnson, and J. L. Bullister (1999), Circulation, mixing, and production of Antarctic Bottom Water, *Prog. Oceanogr.*, *43*, 55–109.

Prinn, R. G., et al. (2000), A history of chemically and radiatively important gases in air deduced from ALE/GAGE/AGAGE, *J. Geophys. Res.*, *105*(D4), 17,751–17,792.

Rehder, G., R. S. Keir, E. Suess, and M. Rhein (1999), Methane in the northern Atlantic controlled by microbial oxidation and atmospheric history, *Geophys. Res. Lett.*, *26*(5), 587–590.

Reid, J. L. (1989), On the total geostrophic circulation of the South Atlantic Ocean: Flow patterns, tracers, and transport, *Prog. Oceanogr.*, *22*, 149–244.

Roether, W. R., R. Schlitzer, A. Putzka, P. Beining, K. Bulsiewicz, G. Rohardt, and F. Delahoyde (1993), A chlorofluoromethane and hydrographic section across Drake Passage: Deep water ventilation and meridional property transport, *J. Geophys. Res.*, *98*(C8), 14,423–14,435.

Sansone, F. J., and C. S. Martens (1978), Methane oxidation in Cape Lookout Bight, North Carolina, *Limnol. Oceanogr.*, *23*, 349–355.

Sansone, F. J., and C. S. Martens (1981), Methane production from acetate and associated methane fluxes from anoxic coastal sediments, *Science*, *211*, 707–709.

Sansone, F. J., B. N. Popp, A. Gasc, A. W. Graham, and T. M. Rust (2001), Highly elevated methane in the eastern tropical North Pacific and associated isotopically enriched fluxes to the atmosphere, *Geophys. Res. Lett.*, *28*(24), 4567–4570.

Schlosser, P., J. L. Bullister, and R. Bayer (1991), Studies of deep water formation and circulation in the Weddell Sea using natural and anthropogenic tracers, *Mar. Chem.*, *35*, 97–122.

Schodlok, M. P., H. H. Hellmer, and A. Beckmann (2002), On the transport, variability and origin of dense water masses crossing the South Scotia Ridge, *Deep Sea Res., Part II*, *49*, 4807–4826.

Scranton, M. I., and P. G. Brewer (1978), Consumption of dissolved methane in the deep ocean, *Limnol. Oceanogr.*, *23*, 1207–1213.

Shine, L. P., Y. Fouquart, V. Ramaswamy, S. Solomon, and J. Srinivasan (1995), Radiative forcing, in *Radiative Forcing of Climate Change*, edited by J. T. Houghton et al., 163–203, Cambridge Univ. Press, New York.

Sieburth, J. M. (1987), Contrary habitats for redox-specific processes: Methanogenesis in oxic waters and oxidation in anoxic waters, in *Microbes in the Sea*, edited by M. A. Sleigh, pp. 11–38, Harwood Acad., New York.

Sueltenfuss, J. (1998), Das Radionuklid Tritium im Ozean: Messverfahren und Verteilung von Tritium im Suedatlantik und im Weddellmeer, *Ber.*, 256.

Suess, E., et al. (1999), Gas hydrate destabilization: enhanced dewatering, benthic material turnover and large methane plumes at the Cascadia convergent margin, *Earth Planet. Sci. Lett.*, *170*, 1–15.

Tilbrook, B. D., and D. M. Karl (1994), Dissolved methane distributions, sources, and sinks in the western Bransfield Strait, Antarctica, *J. Geophys. Res.*, *99*(C8), 16,383–16,393.

Tsunogai, U., N. Yoshida, J. Ishibashi, and T. Gamo (2000), Carbon isotopic distribution of methane in deep sea hydrothermal plume, Myojin Knoll Caldera, Izu-Bonin arc: Implications for microbial methane oxidation in the oceans and applications to heat flux estimation, *Geochim. Cosmochim. Acta*, *64*(14), 2439–2452.

Valentine, D. L., D. C. Blanton, W. S. Reeburgh, and M. Kastner (2001), Water column methane oxidation adjacent to an area of active hydrate dissolution, Eel River Basin, *Geochim. Cosmochim. Acta*, *65*(16), 2633–2640.

Walker, S. J., R. F. Weiss, and R. K. Salameh (2000), Reconstructed histories of the annual mean atmospheric mole fractions for the halocarbons CFC-11, CFC-12, CFC-113 and carbon tetrachloride, *J. Geophys. Res.*, *105*(C6), 14,285–14,296.

Wanninkhof, R. (1992), Relationship between wind speed and gas exchange over the Ocean, *J. Geophys. Res.*, *97*(C5), 7373–7382.

Ward, B. B., and K. A. Kilpatrick (1993), Methane oxidation associated with mid-depth methane maxima in the Southern California Bight, *Cont. Shelf Res.*, *13*(10), 1111–1122.

Ward, B. B., K. A. Kilpatrick, P. C. Novelli, and M. I. Scranton (1987), Methane oxidation and methane fluxes in the ocean surface layer and deep anoxic waters, *Nature*, *327*, 226–229.

Warner, M. J., and R. F. Weiss (1985), Solubilities of chlorofluorocarbons 11 and 12 in water and seawater, *Deep Sea Res.*, *17*, 1479–1485.

Weiss, R. F. (1970), The solubility of nitrogen, oxygen and argon in water and seawater, *Deep Sea Res.*, *17*, 721–735.

Weiss, R. F., H. G. Österlund, and H. Craig (1979), Geochemical studies of the Weddell Sea, *Deep Sea Res., Part A*, *26*, 1093–1120.

Weiss, R. F., J. L. Bullister, R. H. Gammon, and M. J. Warner (1985), Atmospheric chlorofluoromethanes in the deep equatorial Atlantic, *Nature*, *314*, 608–610.

Welhan, J. A., and H. Craig (1983), Methane, hydrogen, and helium in hydrothermal fluids at 21°N on the East Pacific Rise, in *Hydrothermal Processes at Seafloor Spreading Centers*, edited by P. A. Rone, pp. 391–406, Plenum, New York.

Weppernig, R., P. Schlosser, S. Khatiwala, and R. G. Fairbanks (1996), Isotope data from Ice Station Weddell: Implications for deep water formation in the Weddell Sea, *J. Geophys. Res.*, *101*, 25,723–25,739.

Whiticar, M. J. (1999), Carbon and hydrogen isotope systematics of bacterial formation and oxidation of methane, *Chem. Geol.*, *161*, 291–314.

Whitworth, T., III, W. D. Nowlin Jr., A. H. Orsi, R. A. Locarnini, and S. G. Smith (1994), Weddell Sea shelf water in the Bransfield Strait and Weddell-Scotia Confluence, *Deep Sea Res., Part I*, *41*, 629–641.

Wiesenburg, D. A., and N. L. Guinasso Jr. (1979), Equilibrium solubilities of methane, carbon monoxide, and hydrogen in water and sea water, *J. Chem. Eng. Data*, *24*(4), 356–360.

Zyakun, A. M., V. A. Bondar, and B. B. Namsarayev (1979), Fraktsionirovaniye stabil'nööykh izotopov ugleroda metana pri yego mikrobiologicheskom okisleni (Fractionation of stable carbon isotopes in methane during microbiological oxidation), *Geochem. Int.*, *16*, 164–169.

K. U. Heeschen, University of Bremen, Research Center Ocean Margins, P.O. Box 330 440, D-28334 Bremen, Germany. (heeschen@uni-bremen.de)

R. S. Keir, G. Rehder, and E. Suess, Leibniz-Institut für Meereswissenschaften, IFM–GEOMAR, Wischhofstr. 1-3, D-24148 Kiel, Germany. (rkeir@ifm-geomar.de; grehder@ifm-geomar.de; esuess@ifm-geomar.de)

O. Klatt, Alfred Wegener Institute for Polar and Marine Research, Postfach 12 0161, D-27515 Bremerhaven, Germany. (oklatt@awi-bremerhaven.de)

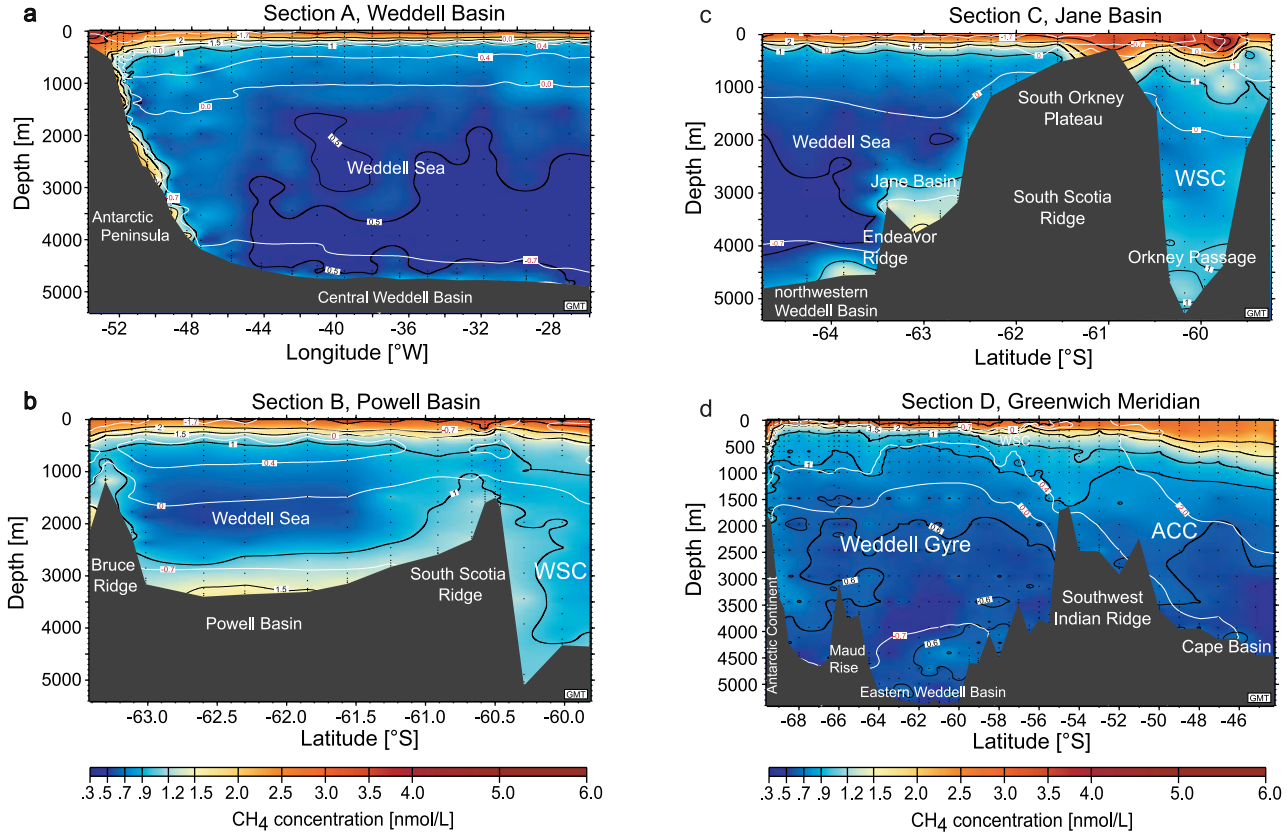

Figure 5. Methane concentrations of four hydrographic sections: (a) along the continental slope of the Antarctic Peninsula and the central Weddell Basin, (b) the Powell Basin and the southern WSC at 48°W, (c) the northwestern Weddell Basin, Jane Basin, South Orkney Shelf, and the WSC at 44°W, and (d) the Weddell Sea, the WSC, and the ACC along the Greenwich Meridian. The white contours show a few major temperature contours (annotation in red; shaded squares in black and white figure), and the black contours show methane concentrations (annotation in black; white boxes in black and white figure).

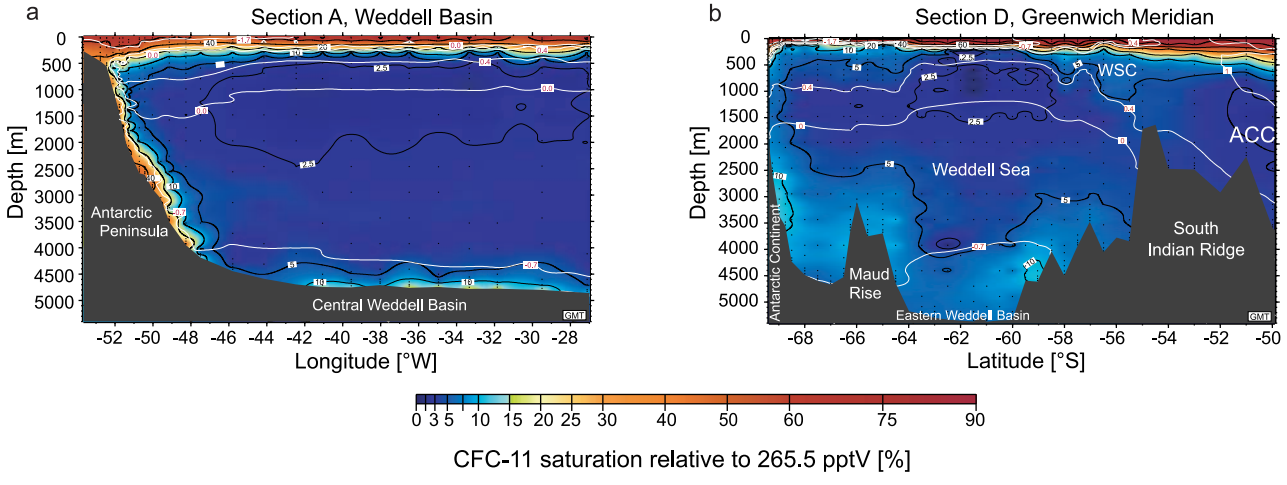

Figure 6. Distribution of dissolved CFC-11, as percentage of saturation with respect to the present atmosphere, along Section A and D [after *Hoppema et al.*, 2001; *Klatt et al.*, 2002]. The white contours show a few major temperature contours (annotation in red; shaded squares in black and white figures), and the black contours show CFC-11 percent saturation (black annotation; white boxes in black and white figure).